https://doi.org/10.5194/egusphere-2022-1382
Preprint. Discussion started: 26 January 2023

Assessment of WRF (v 4.2.1) dynamically downscaled precipitation on subdaily and daily timescales over CONUS

Abhishekh Kumar Srivastava[1], Paul Aaron Ullrich[1], Deeksha Rastogi[2], Pouya Vahmani[3], Andrew Jones[3], and Richard Grotjahn[1]

[1]Department of Land, Air and Water Resources, University of California, Davis, CA, USA.
[2]Computational Science and Engineering Division, Oak Ridge National Laboratory, Oak Ridge, Tennessee, USA.
[3]Climate and Ecosystem Sciences Division, Lawrence Berkeley National Laboratory, CA, USA.

Correspondence: Abhishekh Kumar Srivastava (asrivas@ucdavis.edu)

Abstract. This study analyzes the quality of simulated historical precipitation across the contiguous United States (CONUS) in a 12-km Weather Research and Forecasting model version 4.2.1 (WRF v 4.2.1)-based dynamical downscaling of the fifth generation ECMWF atmospheric reanalysis (ERA5). This work addresses the following questions: First, how well are the 3- and 24-hr precipitation characteristics (diurnal and annual cycles, precipitation frequency, annual and seasonal mean and maximum precipitation, and distribution of seasonal maximum precipitation) represented in the downscaled simulation, compared to ERA5? And second, how does the performance of the simulated WRF precipitation vary across seasons, regions, and timescales? Performance is measured against the NCEP/EMC 4-km Stage IV and PRISM data on 3-hr and 24-hr timescales, respectively. Our analysis suggests that the 12-km WRF exhibits biases typically found in other WRF simulations, including those at convection-permitting scales. In particular, WRF simulates both the timing and magnitude of the summer diurnal precipitation peak as well as ERA5 over most of the CONUS, except for a delayed diurnal peak over the Great Plains. As compared to ERA5, both the month and the magnitude of the precipitation peak annual cycle are remarkably improved in the downscaled WRF simulation. WRF slightly overestimates 3- and 24-hr precipitation maximum over the CONUS, in contrast to ERA5 which generally underestimates these quantities mainly over eastern half of the CONUS. Notably, WRF better captures the probability density distribution (PDF) of 3- and 24-hr annual and seasonal maximum precipitation. WRF exhibits seasonally-dependent precipitation biases across the CONUS, while ERA5's biases are relatively consistent year-round over most of the CONUS. These results suggest that dynamical downscaling to a higher resolution improves upon some precipitation metrics, but is susceptible to common regional climate model biases. Consequently, if used for operational purposes, we suggest moderate bias-correction be applied to the dynamically downscaled product.

https://doi.org/10.5194/egusphere-2022-1382
Preprint. Discussion started: 26 January 2023

1 Introduction

Dynamical downscaling refers to the use of regional climate models forced with initial and lateral boundary conditions derived from either a global climate model or reanalysis to generate high resolution climate output (Giorgi and Mearns, 1991). These high resolution simulations add value through better representation of regional weather and climate phenomena, especially over regions of complex and heterogeneous topography (Doblas-Reyes et al., 2021). For example, better representation of local topography, water bodies and land-sea contrast improves local scale processes such as fine scale convection, land-sea breeze, and nonlinear interactions between local, mesoscale and large-scale processes (Caldwell et al., 2009; Di Luca et al., 2015; Ashfaq et al., 2016; Prein et al., 2016; Bozkurt et al., 2019; Rastogi et al., 2022). The higher resolution and improved representation of physical processes facilitate the studies on future changes in the mean and variability of the weather and climate system (Barsugli et al., 2013) and distilled user-oriented regional climate information on local and regional scales (Rhoades et al., 2020; Doblas-Reyes et al., 2021; Ranasinghe et al., 2021).

Though increased resolution in downscaled climate models is fundamentally important for their utility at regional scales, it is not sufficient for ensuring reliable and accurate information. The biases in regional climate model output are well documented. These biases can originate from various sources, including the lateral boundary conditions (Christensen et al., 2008; Schoetter et al., 2012; Giorgi, 2019) and parameterization schemes (Iguchi et al., 2017; Kong et al., 2022). However, biases are generally not consistent and may vary based on the variable, region and season of interest (Castro et al., 2005; Prein et al., 2015; Diaconescu et al., 2016; Srivastava et al., 2020, 2021, 2022). High resolution and high quality climate data have many uses for both advancing process understanding and for informing operations, particularly at local to regional scales. The ECMWF atmospheric reanalysis (ERA5; Hersbach et al., 2020) represents a great stride forward in the development of a complete historical meteorological dataset with sufficiently high temporal and spatial resolution to represent many forms of extreme weather and their impacts. However, for investigating water resource availability, mountain snowpack, and land-atmosphere fluxes, particularly in the context of multi-sectoral dynamics, even finer grid spacing is required. Given the broad interest among scientists and stakeholders in developing regional climate data products at 1/8° grid spacing based on high-quality reanalysis, it is important to investigate to what degree (if any) the dynamically downscaled data improves upon the original ERA5 product. Such a study is further valuable for informing other dynamical downscaling efforts, such as the international Coordinated Regional Downscaling Experiment (CORDEX) program (Gutowski Jr. et al., 2016).

In this study we evaluate the historical precipitation over the contiguous United States (CONUS) in a 12-km Weather Research and Forecasting model version 4.2.1 (WRF v 4.2.1)-based dynamical downscaling of ERA5 over the period 1980-2020. This WRF-based historical simulation is part of an ensemble data product (Jones et al., 2022) that includes thermodynamic global warming (TGW) simulations under projected climate forcings (Jones et al., in prep). In this paper, we specifically ask: (1) How well are the 3- and 24-hr precipitation characteristics (diurnal and annual cycles, precipitation frequency, annual and seasonal mean and maximum precipitation, and distribution of seasonal maximum precipitation) represented in the downscaled WRF simulation, in comparison to ERA5? (2) How does the performance of the simulated WRF precipitation vary across seasons, regions, and timescales? The performance of 3-hr ERA5 and WRF precipitation simulations are measured against the

https://doi.org/10.5194/egusphere-2022-1382
Preprint. Discussion started: 26 January 2023

NCEP/EMC 4KM Gridded Stage IV Data (Stage IV). The performance of 24-hr ERA5 and WRF precipitation simulations are measured against the Oregon State University Parameter-Elevation Regressions on Independent Slopes Model (PRISM) dataset.

The specific questions above are motivated by several important considerations. Most previous studies have focused on the accuracy of the simulated precipitation on daily or longer timescales (e.g., Bukovsky and Karoly, 2009; Caldwell et al., 2009; Rhoades et al., 2020; Srivastava et al., 2021, 2022; Gensini et al., 2022), likely because of availability of data on daily timescales. However, many of the most high impact precipitation-related physical processes (such as short duration convective storms leading to extreme precipitation events or precipitation intermittency) occur at hourly timescales (Westra et al., 2013; Trenberth et al., 2017), and conclusions drawn from analyzing longer time-scale precipitation do not automatically translate to shorter timescales (Barbero et al., 2019). Further, regional climate models are known to be sensitive to both the resolved (e.g., horizontal resolution and simulation domain) and unresolved parameters (e.g., convection parameterization schemes), and so particular RCM configurations must be examined before they can be used for regional application (Giorgi and Mearns, 1999; Liang et al., 2004). The 12km WRF simulation examined in this study uses a convective parameterization, which is considered to be a major source of model biases on both subdaily and daily timescales (Dirmeyer et al., 2012; Hanel and Buishand, 2010; Knist et al., 2020). Moreover, a seasonal analysis of precipitation is important as generally both the observation-based datasets (e.g., reanalyses) and models (e.g., WRF) better simulate precipitation in winter than in summer, mainly because winter precipitation is mostly dominated by predictable large scale stratiform systems (Ebert et al., 2007) and summer precipitation is mainly influenced by unpredictable small-scale convective cells (Prein et al., 2015; Beck et al., 2019).

The rest of the paper is organized as follows: Section 2 describes the data and methodology used. Results are presented and discussed in section 3 , and also tabulated in Table 1, then summarized in section 4.

2 Data and Method

2.1 WRF downscaling of ERA5

The Weather Research and Forecasting model version 4.2.1 is a state-of-the-art, fully compressible, non-hydrostatic, mesoscale numerical weather prediction system designed for both atmospheric research and operational forecasting applications (Skamarock et al., 2008). For this study, the WRF simulation is carried out at 12-km horizontal grid spacing, and covers the 1980-2020 period (Fig. 1). The physical parameterizations chosen are: Thomson microphysics (Thompson and Eidhammer, 2014), the Tiedke cumulus parameterization (Tiedtke, 1989; Zhang et al., 2011), the Mellor-Yamada-Janjic boundary layer scheme (Janjić, 1994), and the Eta similarity surface layer (Janjić, 1994). Noah is employed for modeling the land surface (Tewari et al., 2004). WRF is further coupled with an urban canopy model (UCM), which resolves urban surfaces, and its land use/land cover is based on National Land Cover Data (NLCD, Dewitz, 2021).

The initial and boundary conditions are obtained from the ERA5 dataset (Hersbach et al., 2020). ERA5 is a fifth generation ECMWF reanalysis product that assimilates a suite of observations (e.g., aircraft, in situ, and satellite) into the Integrated

https://doi.org/10.5194/egusphere-2022-1382
Preprint. Discussion started: 26 January 2023

Forecasting System (IFS) to produce hourly meteorological variables on a regular 0.25 degrees lat-lon grid with 137 vertical levels.

2.1.1 Reference datasets

To evaluate the performance of 3-hr WRF precipitation, NCEP/EMC 4KM Gridded Data Stage IV Data (Stage IV) is used as reference (Lin and Mitchell, 2005). The Stage IV is available at hourly temporal resolution and at 4 km horizontal grid spacing. The Stage IV is generated at NCEP from the regional hourly and 6-hourly multi-sensor (radar + gauges) precipitation analyses produced by the 12 River Forecast Centers (RFCs) over the Continental United States. Beck et al. (2019) report that, to minimize systematic biases in Stage IV data, the dataset is rescaled to match its long-term mean with that of the PRISM dataset (details given below) over the evaluation period (2008–2017).

The performance of 24-hr WRF precipitation is evaluated against the Oregon State University Parameter-Elevation Regressions on Independent Slopes Model (PRISM) dataset at 4km grid spacing (Daly et al., 2008). The daily PRISM data uses in situ data with a digital elevation model to account for the complex meteorological response from orography, rain shadows, temperature inversions, slope aspect, coastal proximity, and other local features.

For comparison, ERA5, Stage IV and PRISM precipitation datasets are interpolated to the 12-km WRF grid using first-order conservative remapping (Jones, 1999).

2.1.2 Diurnal and annual cycle of precipitation

The diurnal cycle of precipitation is estimated by fitting the first two harmonics to the monthly mean 3-hr precipitation. Similarly, the annual cycle of precipitation is estimated by fitting the first two harmonics to the monthly mean 24-hr precipitation. The timing of the diurnal peak of the 3-hr precipitation is expressed in terms of local solar time (LST). LST hours are obtained from UTC hours as follows (Watters et al., 2021):

$$t_{LST} = t_{UTC} + \frac{\lambda^{\circ}}{15^{\circ} h^{-1}}, \tag{1}$$

where, t_{UTC} and t_{LST} are the coordinated universal time and local solar time, respectively. λ is the longitude, in degrees.

In this work, the subdaily precipitation is examined for the 2003-2019 period and the daily precipitation is analyzed for the 2001-2020 period. These periods are chosen for two considerations. First, the hourly Stage IV data are available only after 2002. Second, the variability is assumed to be the same in 20 year period. The results are summarized for the seven National Climate Assessment (NCA) regions over the CONUS (https://www.globalchange.gov/content/nca5-regions). The seven NCA regions are: NW (northwest), SW (southwest), NGP (northern Great Plains), SGP (southern Great Plains), MW (Midwest), SE (southeast), and NE (northeast).

https://doi.org/10.5194/egusphere-2022-1382
Preprint. Discussion started: 26 January 2023

3 Results

3.1 Diurnal cycle of precipitation

Fig. 2 shows the timing of the JJA diurnal precipitation peak in ERA5, WRF and Stage IV datasets (in hours at LST). We chose to analyze the JJA diurnal cycle because the diurnal variations are stronger in summer than in winter (Dai et al., 1999). Presumably this is because winter variations of precipitation are dominated by frontal cyclones and a frontal passage can occur at any time of day thereby masking any diurnal cycle present. During summer, the frontal cyclone passages are much less frequent, allowing the diurnal cycle to be more visible (e.g., Kunkel et al., 2012). The observed (Stage IV) spatial patterns show that, mostly, precipitation peaks in the afternoon over most of the CONUS, except for regions to the east of the Rocky mountains (the Great Plains and MW regions). The eastward propagating shift in nighttime diurnal peak east of the Rockies is consistent with mesoscale convective systems (MCSs) originating over the Rockies and moving eastward (Dai et al., 1999; Tan et al., 2019; Scaff et al., 2020; Watters et al., 2021). ERA5 generally reproduces the spatial pattern of the observed diurnal cycle, but the peak occurs earlier along the northern boundaries of the Northern Great Plains (NGP) and west of the Great Lakes in the Midwest (MW). The largest biases in ERA5 are found between 100°-85°W, also noted in Watters et al. (2021) who compared biases in ERA5 against the Multi-Radar Multi-Sensor (MRMS) gauge-adjusted ground-based radar network product. Similar to ERA5, WRF simulates the observed timing of the diurnal precipitation peak everywhere except over the regions east of the Rockies. Over the regions falling east of 100°W, the observed late night to early morning peak in the diurnal cycle is delayed in the WRF simulation. Similar behavior was also noted in the convection-permitting WRF simulation of Scaff et al. (2020). The slow propagation eastward of convective systems is driven by cloud-scale phenomena that are not necessarily well captured by the models used to generate datasets.

The observed spatial pattern of the diurnal precipitation peak magnitude (precipitation magnitude during the peak of the diurnal cycle) is larger in the eastern CONUS compared to the western CONUS (Fig. 3), with the largest magnitude observed along the Gulf coast and in Florida. ERA5 simulates the observed spatial pattern of the diurnal precipitation magnitude very well. Watters et al. (2021) found that ERA5 generally overestimates the magnitude over much of the CONUS in comparison to the Integrated Multi-satellitE Retrievals for GPM (IMERG) dataset, possibly due to reliance on the convection parameterization. The differing performance of ERA5 against the two different reference datasets (as noted in Watters et al. (2021) and our study) also points to uncertainties arising due to differences in reference datasets. WRF does capture the spatial pattern of the observed diurnal precipitation peak magnitude over most of the CONUS; except over the Southeast where it overestimates the magnitude of the precipitation peak, and over the central Great Plains region where it underestimates the magnitude more than ERA5. The biases in WRF diurnal precipitation magnitude are consistent with those of Scaff et al. (2020), suggesting that current climate models, including WRF, underestimate MCS frequencies in summertime weak synoptic-scale forced conditions (Prein et al., 2020).

https://doi.org/10.5194/egusphere-2022-1382
Preprint. Discussion started: 26 January 2023

3.2 Annual cycle of precipitation

Fig. 4 shows the timing (calendar month) of the monthly averaged precipitation peak (or the annual cycle of the monthly averaged precipitation). Using PRISM as reference, maximum monthly precipitation occurs during winter season over the western CONUS and parts of Arkansas, Mississippi, Louisiana, and the NE CONUS. The majority of the Great Plains is dominated by the late spring and early summer precipitation, whereas the Southeast region gets most of the rainfall in the summer season. This high resolution spatial map of the annual cycle of monthly precipitation is consistent with previous studies (e.g., Bukovsky and Karoly, 2007). Both ERA5 and WRF are able to simulate the spatial pattern of the annual cycle. However, WRF outperforms ERA5 in simulating the spatial structure of the annual cycle, as it greatly improves ERA5 biases over the NE, and parts of the SE and Great Plains regions.

The spatial pattern of the magnitude of the monthly averaged precipitation peak is shown in Fig. 5. The maximum monthly averaged precipitation occurs along the western coast, Sierra Nevada mountains and in the Southeastern region. ERA5 underestimates the precipitation magnitude over the NE and SE regions, and overestimates it over the Southern Great Plains. On the other hand, WRF captures the spatial pattern of the magnitude very well across CONUS, and exhibits much lower biases across the CONUS than ERA5.

In summary, both the timing and magnitude of the monthly averaged precipitation peak show improvement in the downscaled WRF simulation.

3.3 Evaluation of 3-hr precipitation

Fig. 6 shows the precipitation frequency of 3-hr precipitation. The precipitation frequency is computed as the counts of 3-hr precipitation events with magnitude greater than 0.25 mm expressed as a percentage of the total number of 3-hr time steps. Compared with Stage IV, ERA5 overestimates the precipitation frequency by 3–10% in all seasons over most of the CONUS except over the NW and SW. It does underestimate the frequency over the hilly areas of the NW regions in JJA. WRF also exhibits more frequent precipitation mostly over NGP and MW regions in DJF and MAM. In contrast, WRF consistently underestimates precipitation frequency along the west coast. Also, notably, WRF overestimates the frequency over the SE in MAM and JJA and underestimates it in DJF. The spatial pattern of biases in the annual 3-hr precipitation frequency in WRF is consistent with Kong et al. (2022), who found that precipitation frequency in WRF is more sensitive to the convective and radiation schemes than the precipitation amount.

3-hr mean precipitation (mean calculated over all 3-hr time steps) is shown in Fig. 7. From the Stage IV data, the 3-hr mean precipitation is maximum over the coastal and mountainous regions of the western US (Washington, Oregon and Sierra mountains of California). The eastern half of the CONUS experiences more 3-hr average precipitation than the western half (except in the coastal and mountainous regions). The maximum values of Stage IV 3-hr precipitation observed along the northwestern US states are missing in the satellite-derived and bias corrected gridded Climate Prediction Center Morphing technique (CMORPH) dataset, probably due to the insufficient representation of orography at $0.25° \times 0.25°$ grid spacing (Kong et al., 2022). ERA5 generally overestimates the 3-hr mean precipitation over much of the CONUS throughout the year.

https://doi.org/10.5194/egusphere-2022-1382
Preprint. Discussion started: 26 January 2023

On the other hand, while its performance is an improvement in many regions, WRF overestimates the precipitation over most of the CONUS (except SGP) annually or in winter and spring seasons. When compared across seasons, WRF underestimates the summer precipitation but overestimates the winter precipitation over the SGP region. Moreover, WRF simulates a much larger wet bias over the SE in summer than in any other season. The spatial pattern of the WRF simulated precipitation frequency is similar to the mean precipitation amount, suggesting that the subdaily precipitation frequency affects the corresponding subdaily mean precipitation in WRF. The spatial pattern of annual dry bias in the SGP and wet bias in the SE region is also found in the other WRF simulation employing the Tiedke cumulus parameterizatiion scheme along with the Rapid Radiative Transfer Model for global models (RRTMG) radiation scheme (Kong et al., 2022).

The spatial pattern of the 3-hr annual maximum precipitation is shown in Fig. 8. The 3-hr annual maximum precipitation in Stage IV exhibits higher values in the eastern half of the CONUS than in the western half. The spatial pattern and the magnitude in Stage IV is similar to that obtained from the Next-Generation Radar (NEXRAD) dataset in Wehner et al. (2021). ERA5 generally underestimates (mostly within ±5mm) the maximum precipitation in all seasons and everywhere. On the other hand, WRF overestimates the 3-hr annual maximum precipitation over the eastern half of the CONUS, but shows clear seasonal variation in its biases over the western CONUS regions. For example, WRF slightly overestimates the precipitation maxima over parts of the NW, SW, and the GP regions in DJF, but underestimates the maxima over those regions in JJA.

The above analysis of average 3-hr annual maximum precipitation provides little information on whether the datasets reasonably simulate the distribution of the 3-hr annual maximum precipitation. Fig. 9 shows the probability density function (PDF) of the 3-hr annual maximum precipitation. In each panel, the y-axis uses a log-scale to clearly show higher, less frequent precipitation values. It is apparent from the figures that ERA5 consistently underestimates extreme precipitation values over all NCA regions and across all seasons. WRF generally improves on the biases in ERA5 by producing higher extreme precipitation values and thereby bringing the PDF of extreme precipitation values close to the observed PDF.

3.4 Evaluation of 24-hr precipitation

Fig. 10 shows the 24-hr precipitation frequency. The precipitation frequency is computed from the days when 24-hr precipitation is more than 1 mm/day. ERA5 consistently overestimates the 24-hr precipitation frequency by more than 5% in all seasons over most of the CONUS except NW and SW regions. It also underestimates the precipitation frequency over the SW region in summer and fall. In contrast, WRF underestimates the frequency in the NW and SW regions, and shows frequency biases in other regions that are seasonally dependent. For example, over the SE, WRF underestimates the frequency in DJF but overestimates it in JJA. Similarly, WRF overestimates the frequency over NGP and MW in DJF, but it underestimates the frequency over those regions in JJA . It is also notable that WRF underestimates the frequency over most of the CONUS in JJA (except SE) and SON. When compared with the biases in 3-hr precipitation frequency (Fig. 6), the spatial pattern of the biases in ERA5 is similar for both 3-hr and 24-hr precipitation. However, the 24-hr precipitation frequency biases in WRF are larger than those for 3-hr precipitation. This suggests that while ERA5 tends to exhibit more drizzle (i.e., low intensity precipitation), WRF generally concentrates precipitation into fewer days of the year than we see in observations.

https://doi.org/10.5194/egusphere-2022-1382
Preprint. Discussion started: 26 January 2023

Biases in 24-hr precipitation mean are shown in Fig. 11. ERA5 consistently exhibits a dry bias in 24-hr mean precipitation over the Southeast throughout the year. When compared with the frequency biases in Fig. 10, it appears that although ERA5 precipitates more frequently than PRISM, it precipitates less during wet days than PRISM. ERA5 generally exhibits wet biases over other regions. Over the NE, ERA5 shows dry biases over regions close to the coasts and wet biases over the inland areas – a pattern that may be associated with the insufficient ability of ERA5 parameterizations to produce sea breeze-induced precipitation (Crossett et al., 2020). WRF generally shows dry biases over the Great Plains, exhibiting typical model biases existing in the state-of-the-art climate models (Srivastava et al., 2020). The spatial patterns of 24-hr frequency biases in WRF (Fig. 10) are similar to the 24-hr mean precipitation. When compared with ERA5, WRF shows stronger dry biases over the Great Plains regions, particularly in JJA. It is interesting to note that the spatial pattern of the seasonal 24-hr mean precipitation biases in WRF is quite similar to those simulated by another recent bias-corrected convection-permitting WRF simulation over the CONUS (Gensini et al., 2022) – for example, JJA dry biases in both the studies are spread over most the CONUS. Similarly dry biases over the SE region are quite similar. What is more striking is that the magnitude of the 24-hr mean biases in our study are largely comparable to those in Gensini et al. (2022). The summer dry biases in the Great Plains have been reported in previous analyses of WRF simulations employing convection-permitting or convection-parameterizing configurations (Sun et al., 2016), and in other regional climate models, including WRF (Mearns et al., 2012; Gao et al., 2017). The summer dry biases in the Great Plains may be associated with the unrealistically strong coupling of convection with the surface heating over the Rocky Mountains, and insufficiently resolved and slow propagating mesoscale systems (Mearns et al., 2012; Tripathi and Dominguez, 2013; Hu et al., 2018).

Fig. 12 shows biases in 24-hr annual maximum precipitation. ERA5 shows strong and significant dry biases over the eastern CONUS throughout the year. The ERA5 wet biases over the western CONUS are smaller than over the eastern half. These pattern are roughly similar to the 3-hr precipitation biases (Fig. 8). WRF generally shows seasonally-dependent biases across CONUS. For example, it shows wet biases during summer and fall, but a mix of wet and dry biases during winter and spring over the SE. When compared with ERA5, it is evident that though WRF reverses the sign of dry bias over most of the eastern CONUS (except parts of the Great Plains), WRF exhibits smaller magnitude of biases across the CONUS than ERA5.

Finally, the PDF of 24-hr annual maximum precipitation is shown in Fig. 13. It is apparent that ERA5 severely underestimates the annual maximum precipitation across the CONUS and throughout the year. WRF does a much better job of simulating the observed distribution as it reduces the biases in ERA5 frequency distribution of 24-hr annual maximum precipitation for most of the regions and seasons.

For the sake of convenience, the results discussed in this section are also tabulated in Table 1.

4 Summary and discussion

This paper evaluates the performance of the 12-km Weather Research and Forecasting (WRF) based dynamical downscaling of the fifth generation ECMWF atmospheric reanalysis (ERA5) in simulating the subdaily and daily precipitation characteristics. In particular, we evaluate diurnal and annual cycles, frequency and mean precipitation, annual maximum precipitation and its

https://doi.org/10.5194/egusphere-2022-1382
Preprint. Discussion started: 26 January 2023

distribution. We addressed two questions specifically: (1) How well are the 3- and 24-hr precipitation characteristics represented in the downscaled WRF simulation in comparison to those in ERA5? (2) How does the performance of the simulated WRF precipitation vary across seasons, regions, and timescales? We measure the ERA5 and WRF precipitation simulation against the NCEP/EMC 4KM Stage IV and PRSIM data on 3-hr and 24-hr timescales, respectively.

Our analysis suggests that WRF performs similarly to ERA5 in capturing the timing and magnitude of the JJA 3-hr diurnal precipitation peak over most of the CONUS, except the Great Plains regions. Over the Great Plains, WRF exhibits a diurnal cycle delayed by a few hours, suggesting that the mesoscale convective systems, that originate in the Rockies and travel eastward, are slower in the WRF simulation – a typical model problem found in many previous studies. WRF simulates the timing (month) and magnitude of the monthly mean 24-hr precipitation annual cycle much better than ERA5. Notably, WRF improves the timing of the annual cycle over the NE, SE and areas surrounding the Gulf of Mexico. One noticeable difference between ERA5 and WRF is that ERA5 generally displays similar signs of biases (positive or negative) in most of the precipitation characteristics examined throughout the year and across most of the CONUS. However, WRF exhibits seasonally-dependent biases in the precipitation characteristics across the CONUS. For instance, ERA5 overestimates both the frequency and mean of the 3-hr precipitation over most of the CONUS, except over parts of the western CONUS. On the other hand, WRF underestimates the frequency and mean of the 3-hr precipitation over the SE in winter, but overestimates these quantities in summer over that region. Similarly, WRF underestimates the mean 3-hr precipitation over the central Great Plains region in summer, but not in winter. Also, ERA5 generally underpredicts the 3-hr annual and seasonal maximum precipitation throughout the year over the CONUS, but WRF overestimates it over the eastern CONUS in all seasons. What is interesting is that ERA5 performs poorly in simulating the observed probability distribution of the 3-hr precipitation and thus severely underestimates the observed 3-hr extreme precipitation, but WRF performs quite well in capturing the observed PDF, thereby reducing the biases in ERA5. Similar to what was found for the 3-hr precipitation, ERA5 does show similar biases in the 24-hr precipitation, but WRF displays regionally- and seasonally dependent biases. WRF overestimates the 24-hr precipitation frequency over most of the CONUS (except, NW and SW). The 12-km WRF generally exhibits seasonally dependent biases also found in the convection-permitting WRF simulation (Gensini et al., 2022). In this analysis, WRF underestimates the frequency throughout the CONUS in SON, but overestimates the frequency over the eastern half of the CONUS in MAM. The underestimated frequency in WRF is more severe in JJA. Similarly, ERA5 underestimates the 24-hr annual maximum precipitation over the eastern half of the CONUS, most notably in the Great Plains and SE regions; whereas, these biases are generally reduced in magnitude in the WRF simulation, but they also occur with a change in the sign. Notably, ERA5 underestimates the 24-hr annual maximum precipitation over the SE, while WRF overestimates it (though by a smaller overall magnitude). As observed for 3-hr precipitation, WRF shows remarkable improvements in the simulated probability distribution of the 24-hr annual maximum precipitation; throughout the CONUS, ERA5 does have problems in capturing the extreme precipitation magnitudes, suggesting that its representation of the strongest precipitation extremes is overly conservative. These results are also summarized in Table 1.

This work adds to the literature addressing the value of dynamical downscaling to higher resolution. Our results echo similar past studies, which generally show a mixture of improvement and deterioration in the quality of simulated fields. Although we

https://doi.org/10.5194/egusphere-2022-1382
Preprint. Discussion started: 26 January 2023

find that dynamical downscaling with WRF simulates observed precipitation characteristics reasonably well on both the daily and subdaily timescales, improvements do not emerge everywhere. Particularly, WRF exhibits several common biases found in many other models, which are likely suppressed in ERA5 through data assimilation. As hypothesized in this study, WRF does show seasonally- and regionally- dependent biases in precipitation, while ERA5's biases are less seasonal. Nonetheless, WRF greatly improves upon the PDFs of annual maximum precipitation at both 3-hr and 24-hr timescales, and improves on the month and magnitude of the seasonal precipitation cycle. This suggests the WRF product is generally more useful when it comes to its representation of precipitation extremes – which seems to be a consequence of the fact WRF tends to produce generally flashier precipitation. These results suggest care should be taken in using the WRF simulations for further applications such as future regional climate projections or regional hydrologic modeling.

While the 12km grid spacing of these simulations is a clear refinement on the native resolution of ERA5, ultimately it would be far more desirable to run the downscaled simulation in the convection-resolving regime (i.e., 3km or finer). We expect the match between the precipitation frequency distribution in the tail will improve monotonically with resolution. Until convection-resolving scales are reached, important processes such as horizontal propagation of mesoscale convective systems will not be properly represented. Consequently, when it becomes possible to reach these spatial scales at climatological time scales with available computing power, we would advocate for the metrics explored in this study to be revisited.

Code and data availability. The WRF source code is available on GitHub: https://github.com/wrf-model. ERA5 is publicly accessible from https://www.ecmwf.int/en/forecasts/datasets/reanalysis-datasets/era5. PRISM precipitation data can be downloaded from https://prism.oregonstate.edu/, and Stage IV data is available on https://data.eol.ucar.edu/dataset/21.093. WRF data is accessible at https://data.msdlive.org/records/ksw6r-2xv06. The 40-year historical WRF dataset can be downloaded from https://data.msdlive.org/records/ksw6r-2xv06.

Author contributions. Abhishekh Kumar Srivastava: Conceptualization; Methodology; Software; Validation; Formal analysis; Investigation; Writing - original draft, review & editing. Paul A. Ullrich: Conceptualization; Validation; Resources; Writing - original draft, review & editing; Supervision; Project administration; Funding acquisition; Deeksha Rastogi, Pouya Vahamani and Andrew Jones: Model Simulation; Writing - review & editing. Richard Grotjahn: Writing - original draft, review & editing; Supervision.

Competing interests. The authors declare that they have no known competing financial interests.

Acknowledgements. This work is supported by the Department of Energy Office of Science award number DE-SC0016605, "A Framework for Improving Analysis and Modeling of Earth System and Intersectoral Dynamics at Regional Scales." The climate forcing for this paper was developed collaboratively between the IM3 and HyperFACETS projects, both of which are supported by the U.S. Department of Energy, Office of Science, as part of research in MultiSector Dynamics, and Regional and Global Model Analysis, Earth and Environmental System

https://doi.org/10.5194/egusphere-2022-1382
Preprint. Discussion started: 26 January 2023

Modeling Program. A portion of this research used the computing resources of the National Energy Research Scientific Computing Center (NERSC), a U.S. Department of Energy Office of Science User Facility located at Lawrence Berkeley National Laboratory, operated under Contract No. DE-AC02-05CH11231. DR is an employee of UT-Battelle, LLC, under contract DEAC05-00OR22725 with the US Department of Energy (DOE). Accordingly, the publisher, by accepting the article for publication, acknowledges that the US government retains a nonexclusive, paid-up, irrevocable, worldwide license to publish or reproduce the published form of this manuscript, or allow others to do so, for US government purposes. DOE will provide public access to these results of federally sponsored research in accordance with the DOE Public Access Plan (https://www.energy.gov/downloads/doe-public-access-plan).

https://doi.org/10.5194/egusphere-2022-1382
Preprint. Discussion started: 26 January 2023

References

Ashfaq, M., Rastogi, D., Mei, R., Kao, S.-C., Gangrade, S., Naz, B. S., and Touma, D.: High-resolution ensemble projections of near-term regional climate over the continental United States, Journal of Geophysical Research: Atmospheres, 121, 9943–9963, https://doi.org/https://doi.org/10.1002/2016JD025285, 2016.

Barbero, R., Fowler, H. J., Blenkinsop, S., Westra, S., Moron, V., Lewis, E., Chan, S., Lenderink, G., Kendon, E., Guerreiro, S., Li, X.-F., Villalobos, R., Ali, H., and Mishra, V.: A synthesis of hourly and daily precipitation extremes in different climatic regions, Weather and Climate Extremes, 26, 100 219, https://doi.org/https://doi.org/10.1016/j.wace.2019.100219, 2019.

Barsugli, J. J., Guentchev, G., Horton, R. M., Wood, A., Mearns, L. O., Liang, X.-Z., Winkler, J. A., Dixon, K., Hayhoe, K., Rood, R. B., Goddard, L., Ray, A., Buja, L., and Ammann, C.: The Practitioner's Dilemma: How to Assess the Credibility of Downscaled Climate Projections, Eos, Transactions American Geophysical Union, 94, 424–425, https://doi.org/https://doi.org/10.1002/2013EO460005, 2013.

Beck, H. E., Pan, M., Roy, T., Weedon, G. P., Pappenberger, F., van Dijk, A. I. J. M., Huffman, G. J., Adler, R. F., and Wood, E. F.: Daily evaluation of 26 precipitation datasets using Stage-IV gauge-radar data for the CONUS, Hydrology and Earth System Sciences, 23, 207–224, https://doi.org/10.5194/hess-23-207-2019, 2019.

Bozkurt, D., Rojas, M., Boisier, J. P., Rondanelli, R., Garreaud, R., and Gallardo, L.: Dynamical downscaling over the complex terrain of southwest South America: present climate conditions and added value analysis, Climate Dynamics, 53, 6745–6767, https://doi.org/https://doi.org/10.1007/s00382-019-04959-y, 2019.

Bukovsky, M. S. and Karoly, D. J.: A Brief Evaluation of Precipitation from the North American Regional Reanalysis, Journal of Hydrometeorology, 8, 837 – 846, https://doi.org/10.1175/JHM595.1, 2007.

Bukovsky, M. S. and Karoly, D. J.: Precipitation Simulations Using WRF as a Nested Regional Climate Model, Journal of Applied Meteorology and Climatology, 48, 2152 – 2159, https://doi.org/10.1175/2009JAMC2186.1, 2009.

Caldwell, P., Chin, H.-N. S., Bader, D. C., and Bala, G.: Evaluation of a WRF dynamical downscaling simulation over California, Climatic change, 95, 499–521, 2009.

Castro, C. L., Pielke Sr., R. A., and Leoncini, G.: Dynamical downscaling: Assessment of value retained and added using the Regional Atmospheric Modeling System (RAMS), Journal of Geophysical Research: Atmospheres, 110, https://doi.org/https://doi.org/10.1029/2004JD004721, 2005.

Christensen, J. H., Boberg, F., Christensen, O. B., and Lucas-Picher, P.: On the need for bias correction of regional climate change projections of temperature and precipitation, Geophysical Research Letters, 35, https://doi.org/10.1029/2008GL035694, 2008.

Crossett, C. C., Betts, A. K., Dupigny-Giroux, L.-A. L., and Bomblies, A.: Evaluation of Daily Precipitation from the ERA5 Global Reanalysis against GHCN Observations in the Northeastern United States, Climate, 8, https://doi.org/10.3390/cli8120148, 2020.

Dai, A., Giorgi, F., and Trenberth, K. E.: Observed and model-simulated diurnal cycles of precipitation over the contiguous United States, Journal of Geophysical Research: Atmospheres, 104, 6377–6402, https://doi.org/https://doi.org/10.1029/98JD02720, 1999.

Daly, C., Halbleib, M., Smith, J. I., Gibson, W. P., Doggett, M. K., Taylor, G. H., Curtis, J., and Pasteris, P. P.: Physiographically sensitive mapping of climatological temperature and precipitation across the conterminous United States, International Journal of Climatology, 28, 2031–2064, https://doi.org/10.1002/joc.1688, 2008.

Dewitz, J.: National Land Cover Database (NLCD) 2019 Products [Dataset], US Geological Survey: Sioux Falls, SD, USA, https://doi.org/10.5066/P9KZCM54, 2021.

350 Di Luca, A., de Elía, R., and Laprise, R.: Challenges in the quest for added value of regional climate dynamical downscaling, Current Climate Change Reports, 1, 10–21, 2015.

Diaconescu, E. P., Gachon, P., Laprise, R., and Scinocca, J. F.: Evaluation of Precipitation Indices over North America from Various Configurations of Regional Climate Models, Atmosphere-Ocean, 54, 418–439, https://doi.org/10.1080/07055900.2016.1185005, 2016.

Dirmeyer, P. A., Cash, B. A., Kinter, J. L., Jung, T., Marx, L., Satoh, M., Stan, C., Tomita, H., Towers, P., Wedi, N., et al.: Simulating the diurnal cycle of rainfall in global climate models: Resolution versus parameterization, Climate dynamics, 39, 399–418, https://doi.org/https://doi.org/10.1007/s00382-011-1127-9, 2012.

Doblas-Reyes, F. J., Sörensson, A. A., Almazroui, M., Dosio, A., Gutowski, W. J., Haarsma, R., Hamdi, R., Hewitson, B., Kwon, W.-T., Lamptey, B. L., Maraun, D., Stephenson, T. S., Takayabu, I., Terray, L., Turner, A., and Zuo, Z.: Linking Global to Regional Climate Change, book section 10, p. 1363–1512, Cambridge University Press, Cambridge, United Kingdom and New York, NY, USA, https://doi.org/10.1017/9781009157896.012, 2021.

Ebert, E. E., Janowiak, J. E., and Kidd, C.: Comparison of Near-Real-Time Precipitation Estimates from Satellite Observations and Numerical Models, Bulletin of the American Meteorological Society, 88, 47 – 64, https://doi.org/10.1175/BAMS-88-1-47, 2007.

Gao, Y., Leung, L. R., Zhao, C., and Hagos, S.: Sensitivity of U.S. summer precipitation to model resolution and convective parameterizations across gray zone resolutions, Journal of Geophysical Research: Atmospheres, 122, 2714–2733, https://doi.org/https://doi.org/10.1002/2016JD025896, 2017.

Gensini, V. A., Haberlie, A. M., and Ashley, W. S.: Convection-permitting simulations of historical and possible future climate over the contiguous United States, Climate Dynamics, pp. 1–18, https://doi.org/https://doi.org/10.1007/s00382-022-06306-0, 2022.

Giorgi, F.: Thirty Years of Regional Climate Modeling: Where Are We and Where Are We Going next?, Journal of Geophysical Research: Atmospheres, 124, 5696–5723, https://doi.org/10.1029/2018JD030094, 2019.

370 Giorgi, F. and Mearns, L. O.: Approaches to the simulation of regional climate change: A review, Reviews of Geophysics, 29, 191–216, https://doi.org/10.1029/90RG02636, 1991.

Giorgi, F. and Mearns, L. O.: Introduction to special section: Regional Climate Modeling Revisited, Journal of Geophysical Research: Atmospheres, 104, 6335–6352, https://doi.org/https://doi.org/10.1029/98JD02072, 1999.

Gutowski Jr., W. J., Giorgi, F., Timbal, B., Frigon, A., Jacob, D., Kang, H.-S., Raghavan, K., Lee, B., Lennard, C., Nikulin, G., O'Rourke, E., Rixen, M., Solman, S., Stephenson, T., and Tangang, F.: WCRP COordinated Regional Downscaling EXperiment (CORDEX): a diagnostic MIP for CMIP6, Geoscientific Model Development, 9, 4087–4095, https://doi.org/10.5194/gmd-9-4087-2016, 2016.

Hanel, M. and Buishand, T. A.: On the value of hourly precipitation extremes in regional climate model simulations, Journal of hydrology, 393, 265–273, 2010.

Hersbach, H., Bell, B., Berrisford, P., Hirahara, S., Horányi, A., Muñoz-Sabater, J., Nicolas, J., Peubey, C., Radu, R., Schepers, D., Simmons, A., Soci, C., Abdalla, S., Abellan, X., Balsamo, G., Bechtold, P., Biavati, G., Bidlot, J., Bonavita, M., De Chiara, G., Dahlgren, P., Dee, D., Diamantakis, M., Dragani, R., Flemming, J., Forbes, R., Fuentes, M., Geer, A., Haimberger, L., Healy, S., Hogan, R. J., Hólm, E., Janisková, M., Keeley, S., Laloyaux, P., Lopez, P., Lupu, C., Radnoti, G., de Rosnay, P., Rozum, I., Vamborg, F., Villaume, S., and Thépaut, J.-N.: The ERA5 global reanalysis, Quarterly Journal of the Royal Meteorological Society, 146, 1999–2049, https://doi.org/10.1002/qj.3803, 2020.

385 Hu, X.-M., Xue, M., McPherson, R. A., Martin, E., Rosendahl, D. H., and Qiao, L.: Precipitation Dynamical Downscaling Over the Great Plains, Journal of Advances in Modeling Earth Systems, 10, 421–447, https://doi.org/https://doi.org/10.1002/2017MS001154, 2018.

https://doi.org/10.5194/egusphere-2022-1382
Preprint. Discussion started: 26 January 2023

Iguchi, T., Tao, W.-K., Wu, D., Peters-Lidard, C., Santanello, J. A., Kemp, E., Tian, Y., Case, J., Wang, W., Ferraro, R., Waliser, D., Kim, J., Lee, H., Guan, B., Tian, B., and Loikith, P.: Sensitivity of CONUS Summer Rainfall to the Selection of Cumulus Parameterization Schemes in NU-WRF Seasonal Simulations, Journal of Hydrometeorology, 18, 1689 – 1706, https://doi.org/10.1175/JHM-D-16-0120.1, 2017.

Janjić, Z. I.: The Step-Mountain Eta Coordinate Model: Further Developments of the Convection, Viscous Sublayer, and Turbulence Closure Schemes, Monthly Weather Review, 122, 927 – 945, https://doi.org/10.1175/1520-0493(1994)122<0927:TSMECM>2.0.CO;2, 1994.

Jones, A. D., Rastogi, D., Vahmani, P., Stansfield, A., Reed, K., Thurber, T., Ullrich, P., and Rice, J. S.: Climate projections for the continental United States based on thermodynamic modification of historic weather.

Jones, A. D., Rastogi, D., Vahmani, P., Stansfield, A., Reed, K., Ullrich, P., and Rice, J. S.: IM3/HyperFACETS Thermodynamic Global Warming (TGW) Simulation Datasets (v1.0.0), Tech. rep., MultiSector Dynamics-Living, Intuitive, Value-adding, Environment, https://doi.org/https://doi.org/10.57931/1885756, 2022.

Jones, P. W.: First- and Second-Order Conservative Remapping Schemes for Grids in Spherical Coordinates, Monthly Weather Review, 127, 2204–2210, https://doi.org/10.1175/1520-0493(1999)127<2204:FASOCR>2.0.CO;2, 1999.

Knist, S., Goergen, K., and Simmer, C.: Evaluation and projected changes of precipitation statistics in convection-permitting WRF climate simulations over Central Europe, Climate Dynamics, 55, 325–341, https://doi.org/https://doi.org/10.1007/s00382-018-4147-x, 2020.

Kong, X., Wang, A., Bi, X., Sun, B., and Wei, J.: The Hourly Precipitation Frequencies in the Tropical-Belt Version of WRF: Sensitivity to Cumulus Parameterization and Radiation Schemes, Journal of Climate, 35, 285 – 304, https://doi.org/10.1175/JCLI-D-20-0854.1, 2022.

Kunkel, K. E., Easterling, D. R., Kristovich, D. A. R., Gleason, B., Stoecker, L., and Smith, R.: Meteorological Causes of the Secular Variations in Observed Extreme Precipitation Events for the Conterminous United States, Journal of Hydrometeorology, 13, 1131 – 1141, https://doi.org/10.1175/JHM-D-11-0108.1, 2012.

Liang, X.-Z., Li, L., Kunkel, K. E., Ting, M., and Wang, J. X. L.: Regional Climate Model Simulation of U.S. Precipitation during 1982–2002. Part I: Annual Cycle, Journal of Climate, 17, 3510 – 3529, https://doi.org/10.1175/1520-0442(2004)017<3510:RCMSOU>2.0.CO;2, 2004.

Lin, Y. and Mitchell, K. E.: 1.2 the NCEP stage II/IV hourly precipitation analyses: Development and applications, in: Proceedings of the 19th Conference Hydrology, American Meteorological Society, San Diego, CA, USA, vol. 10, Citeseer, 2005.

Mearns, L. O., Arritt, R., Biner, S., Bukovsky, M. S., McGinnis, S., Sain, S., Caya, D., Correia, J., Flory, D., Gutowski, W., Takle, E. S., Jones, R., Leung, R., Moufouma-Okia, W., McDaniel, L., Nunes, A. M. B., Qian, Y., Roads, J., Sloan, L., and Snyder, M.: The North American Regional Climate Change Assessment Program: Overview of Phase I Results, Bulletin of the American Meteorological Society, 93, 1337 – 1362, https://doi.org/10.1175/BAMS-D-11-00223.1, 2012.

Prein, A., Gobiet, A., Truhetz, H., Keuler, K., Goergen, K., Teichmann, C., Maule, C. F., Van Meijgaard, E., Déqué, M., Nikulin, G., et al.: Precipitation in the EURO-CORDEX 0.11° and 0.44° simulations: high resolution, high benefits?, Climate dynamics, 46, 383–412, 2016.

Prein, A. F., Langhans, W., Fosser, G., Ferrone, A., Ban, N., Goergen, K., Keller, M., Tölle, M., Gutjahr, O., Feser, F., Brisson, E., Kollet, S., Schmidli, J., van Lipzig, N. P. M., and Leung, R.: A review on regional convection-permitting climate modeling: Demonstrations, prospects, and challenges, Reviews of Geophysics, 53, 323–361, https://doi.org/https://doi.org/10.1002/2014RG000475, 2015.

Prein, A. F., Liu, C., Ikeda, K., Bullock, R., Rasmussen, R. M., Holland, G. J., and Clark, M.: Simulating North American mesoscale convective systems with a convection-permitting climate model, Climate Dynamics, 55, 95–110, https://doi.org/https://doi.org/10.1007/s00382-017-3993-2, 2020.

Ranasinghe, R., Ruane, A., Vautard, R., Arnell, N., Coppola, E., Cruz, F., Dessai, S., Islam, A., Rahimi, M., Ruiz Carrascal, D., Sillmann, J., Sylla, M., Tebaldi, C., Wang, W., and Zaaboul, R.: Climate Change Information for Regional Impact and for Risk Assessment, book section 12, p. 1767–1926, Cambridge University Press, Cambridge, United Kingdom and New York, NY, USA, https://doi.org/10.1017/9781009157896.014, 2021.

Rastogi, D., Kao, S.-C., and Ashfaq, M.: How May the Choice of Downscaling Techniques and Meteorological Reference Observations Affect Future Hydroclimate Projections?, Earth's Future, 10, e2022EF002 734, https://doi.org/https://doi.org/10.1029/2022EF002734, e2022EF002734 2022EF002734, 2022.

Rhoades, A. M., Jones, A. D., Srivastava, A., Huang, H., O'Brien, T. A., Patricola, C. M., Ullrich, P. A., Wehner, M., and Zhou, Y.: The Shifting Scales of Western U.S. Landfalling Atmospheric Rivers Under Climate Change, Geophysical Research Letters, 47, e2020GL089 096, https://doi.org/https://doi.org/10.1029/2020GL089096, e2020GL089096 10.1029/2020GL089096, 2020.

Scaff, L., Prein, A. F., Li, Y., Liu, C., Rasmussen, R., and Ikeda, K.: Simulating the convective precipitation diurnal cycle in North America's current and future climate, Climate Dynamics, 55, 369–382, https://doi.org/https://doi.org/10.1007/s00382-019-04754-9, 2020.

Schoetter, R., Hoffmann, P., Rechid, D., and Schlünzen, K. H.: Evaluation and Bias Correction of Regional Climate Model Results Using Model Evaluation Measures, Journal of Applied Meteorology and Climatology, 51, 1670–1684, https://doi.org/10.1175/JAMC-D-11-0161.1, 2012.

Skamarock, W. C., Klemp, J. B., Dudhia, J., Gill, D. O., Barker, D., Duda, M. G., Huang, X., Wang, W., and Powers, J. G.: A Description of the Advanced Research WRF Version 3 (No. NCAR/TN-475+STR), https://doi.org/http://dx.doi.org/10.5065/D68S4MVH, 2008.

Srivastava, A., Grotjahn, R., and Ullrich, P. A.: Evaluation of historical CMIP6 model simulations of extreme precipitation over contiguous US regions, Weather and Climate Extremes, 29, 100 268, https://doi.org/https://doi.org/10.1016/j.wace.2020.100268, 2020.

Srivastava, A. K., Grotjahn, R., Ullrich, P. A., and Sadegh, M.: Pooling Data Improves Multimodel IDF Estimates over Median-Based IDF Estimates: Analysis over the Susquehanna and Florida, Journal of Hydrometeorology, 22, 971–995, https://doi.org/https://doi.org/10.1175/JHM-D-20-0180.1, 2021.

Srivastava, A. K., Grotjahn, R., Ullrich, P. A., and Zarzycki, C.: Evaluation of precipitation indices in suites of dynamically and statistically downscaled regional climate models over Florida, Climate Dynamics, 58, 1587–1611, https://doi.org/https://doi.org/10.1007/s00382-021-05980-w, 2022.

Sun, X., Xue, M., Brotzge, J., McPherson, R. A., Hu, X.-M., and Yang, X.-Q.: An evaluation of dynamical downscaling of Central Plains summer precipitation using a WRF-based regional climate model at a convection-permitting 4 km resolution, Journal of Geophysical Research: Atmospheres, 121, 13,801–13,825, https://doi.org/https://doi.org/10.1002/2016JD024796, 2016.

Tan, J., Huffman, G. J., Bolvin, D. T., and Nelkin, E. J.: Diurnal Cycle of IMERG V06 Precipitation, Geophysical Research Letters, 46, 13 584–13 592, https://doi.org/https://doi.org/10.1029/2019GL085395, 2019.

Tewari, M., N., Chen, F., Wang, W., Dudhia, J., LeMone, M., Mitchell, K., Ek, M., Gayno, G., Wegiel, J., et al.: Implementation and verification of the unified NOAH land surface model in the WRF model (Formerly Paper Number 17.5), in: Proceedings of the 20th Conference on Weather Analysis and Forecasting/16th Conference on Numerical Weather Prediction, Seattle, WA, USA, vol. 14, 2004.

Thompson, G. and Eidhammer, T.: A Study of Aerosol Impacts on Clouds and Precipitation Development in a Large Winter Cyclone, Journal of the Atmospheric Sciences, 71, 3636 – 3658, https://doi.org/10.1175/JAS-D-13-0305.1, 2014.

Tiedtke, M.: A Comprehensive Mass Flux Scheme for Cumulus Parameterization in Large-Scale Models, Monthly Weather Review, 117, 1779 – 1800, https://doi.org/10.1175/1520-0493(1989)117<1779:ACMFSF>2.0.CO;2, 1989.

https://doi.org/10.5194/egusphere-2022-1382
Preprint. Discussion started: 26 January 2023

Trenberth, K. E., Zhang, Y., and Gehne, M.: Intermittency in Precipitation: Duration, Frequency, Intensity, and Amounts Using Hourly Data, Journal of Hydrometeorology, 18, 1393 – 1412, https://doi.org/10.1175/JHM-D-16-0263.1, 2017.

Tripathi, O. P. and Dominguez, F.: Effects of spatial resolution in the simulation of daily and subdaily precipitation in the southwestern US, Journal of Geophysical Research: Atmospheres, 118, 7591–7605, https://doi.org/https://doi.org/10.1002/jgrd.50590, 2013.

Watters, D., Battaglia, A., and Allan, R. P.: The Diurnal Cycle of Precipitation according to Multiple Decades of Global Satellite Observations, Three CMIP6 Models, and the ECMWF Reanalysis, Journal of Climate, 34, 5063 – 5080, https://doi.org/10.1175/JCLI-D-20-0966.1, 2021.

Wehner, M., Lee, J., Risser, M., Ullrich, P., Gleckler, P., and Collins, W. D.: Evaluation of extreme sub-daily precipitation in high-resolution global climate model simulations, Philosophical Transactions of the Royal Society A: Mathematical, Physical and Engineering Sciences, 379, 20190 545, https://doi.org/10.1098/rsta.2019.0545, 2021.

Westra, S., Alexander, L. V., and Zwiers, F. W.: Global Increasing Trends in Annual Maximum Daily Precipitation, Journal of Climate, 26, 3904–3918, https://doi.org/10.1175/JCLI-D-12-00502.1, 2013.

Zhang, C., Wang, Y., and Hamilton, K.: Improved Representation of Boundary Layer Clouds over the Southeast Pacific in ARW-WRF Using a Modified Tiedtke Cumulus Parameterization Scheme, Monthly Weather Review, 139, 3489 – 3513, https://doi.org/10.1175/MWR-D-10-05091.1, 2011.

https://doi.org/10.5194/egusphere-2022-1382
Preprint. Discussion started: 26 January 2023

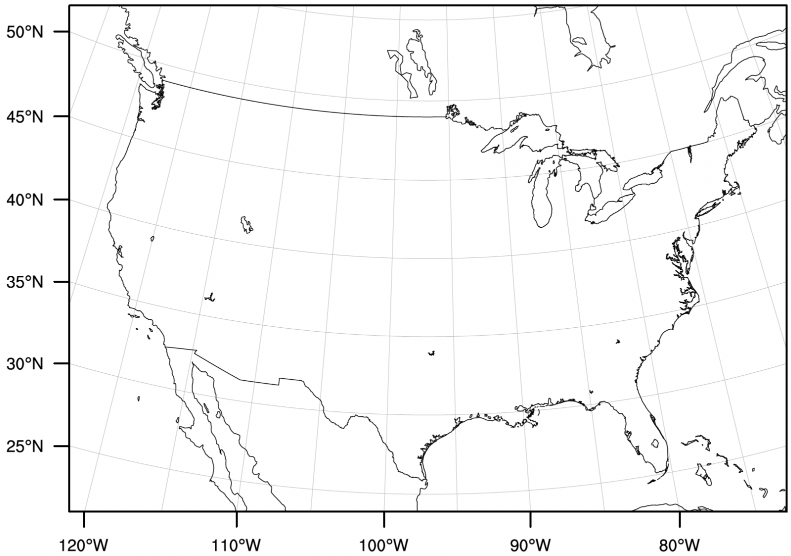

Figure 1. The WRF domain employed in this study.

https://doi.org/10.5194/egusphere-2022-1382
Preprint. Discussion started: 26 January 2023

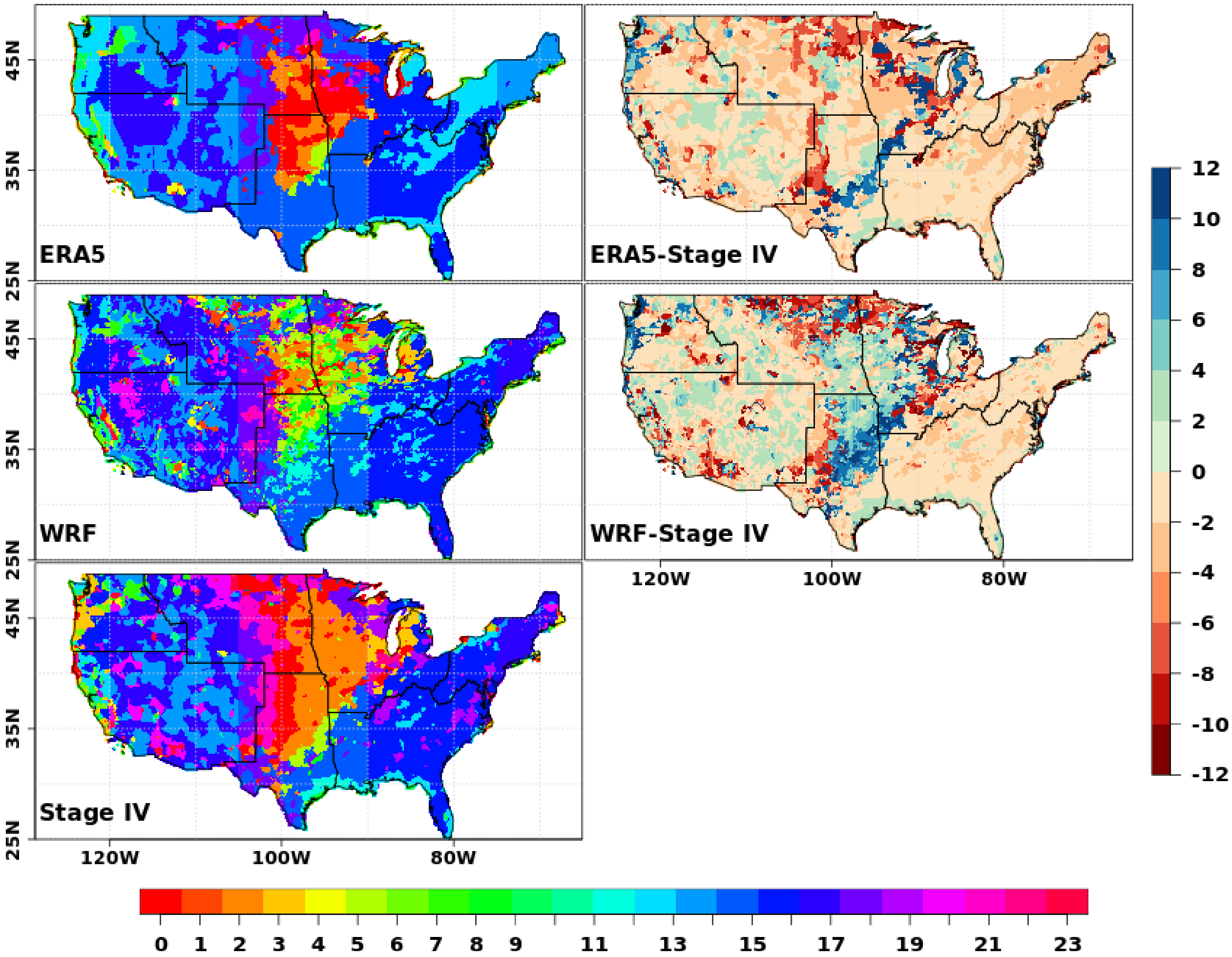

Figure 2. Timing of the diurnal precipitation peak in JJA (in units of hours at local solar time) estimated over 2003-2019. The left column shows the timing in each dataset and uses the color scale along the bottom edge of the figure. The right column shows differences in timings of the precipitation peak and uses the color scale along the right edge of the figure.

https://doi.org/10.5194/egusphere-2022-1382
Preprint. Discussion started: 26 January 2023

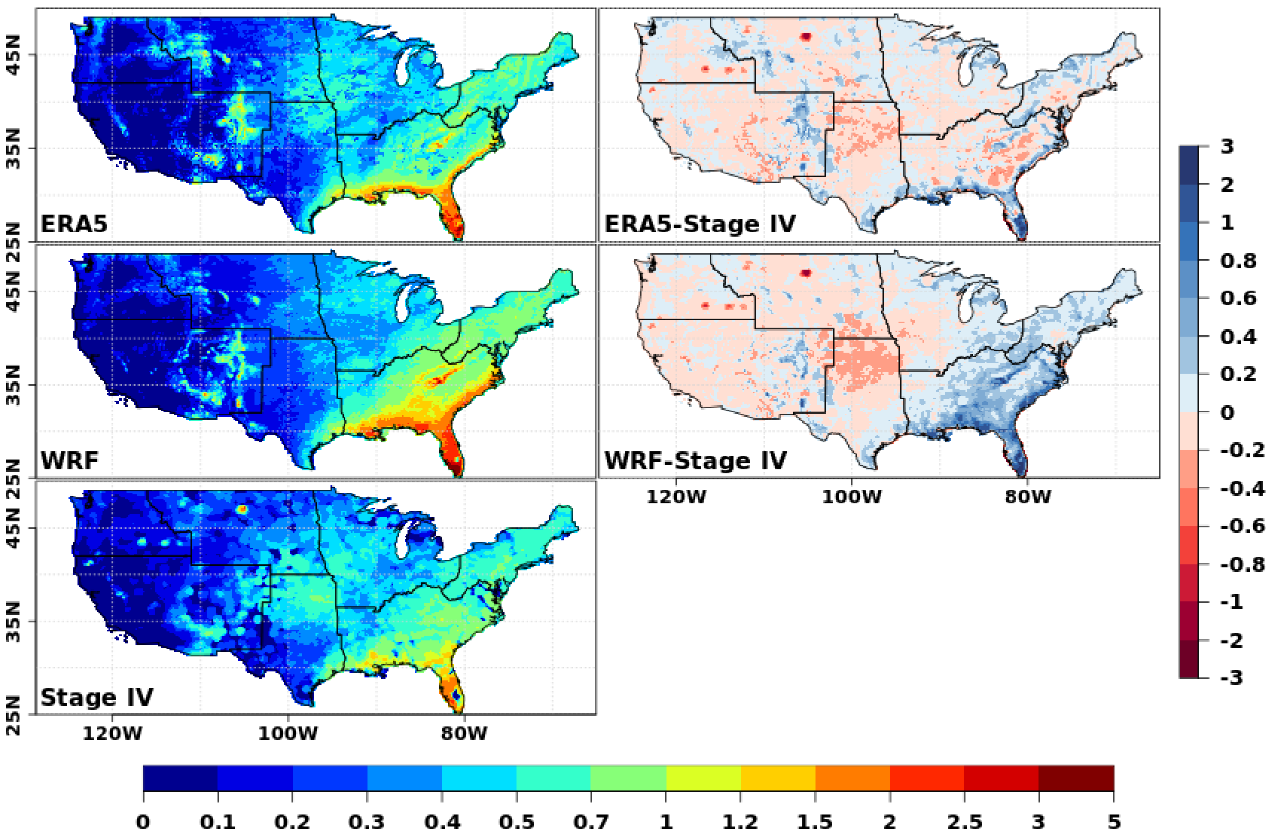

Figure 3. Magnitude of the diurnal precipitation peak in JJA estimated over 2003-2019. The left column shows the magnitude in each dataset and uses the color scale along the bottom edge of the figure. The right column shows biases in the magnitude of the precipitation peak and uses the color scale along the right edge of the figure. Units: mm/3hr

https://doi.org/10.5194/egusphere-2022-1382
Preprint. Discussion started: 26 January 2023

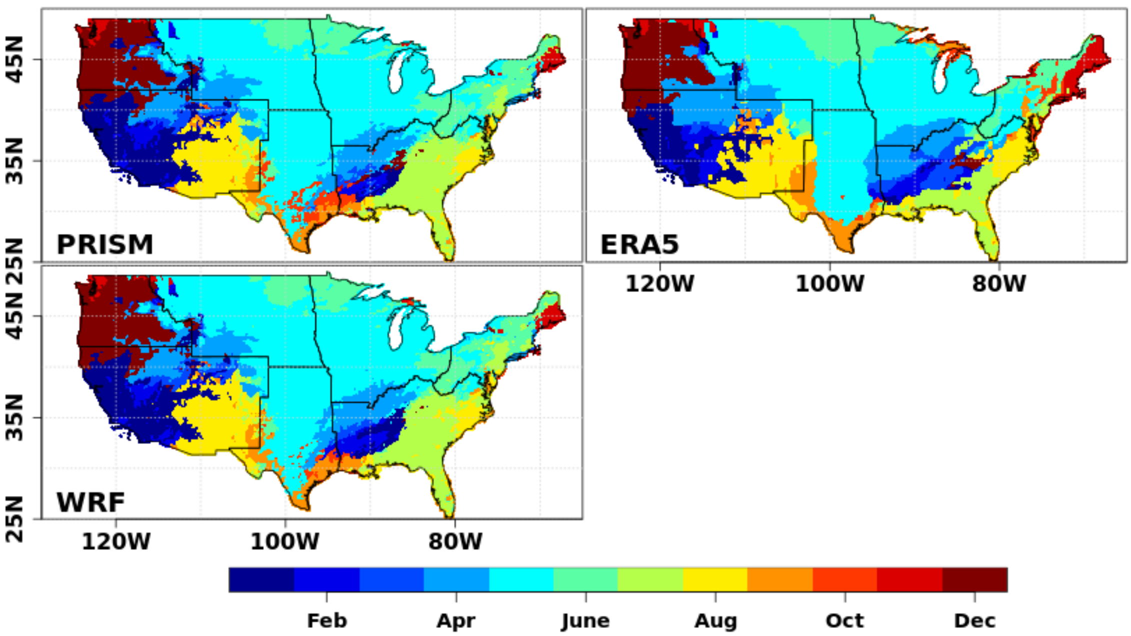

Figure 4. Calendar month of the monthly average precipitation peak estimated over 2001-2020.

https://doi.org/10.5194/egusphere-2022-1382
Preprint. Discussion started: 26 January 2023

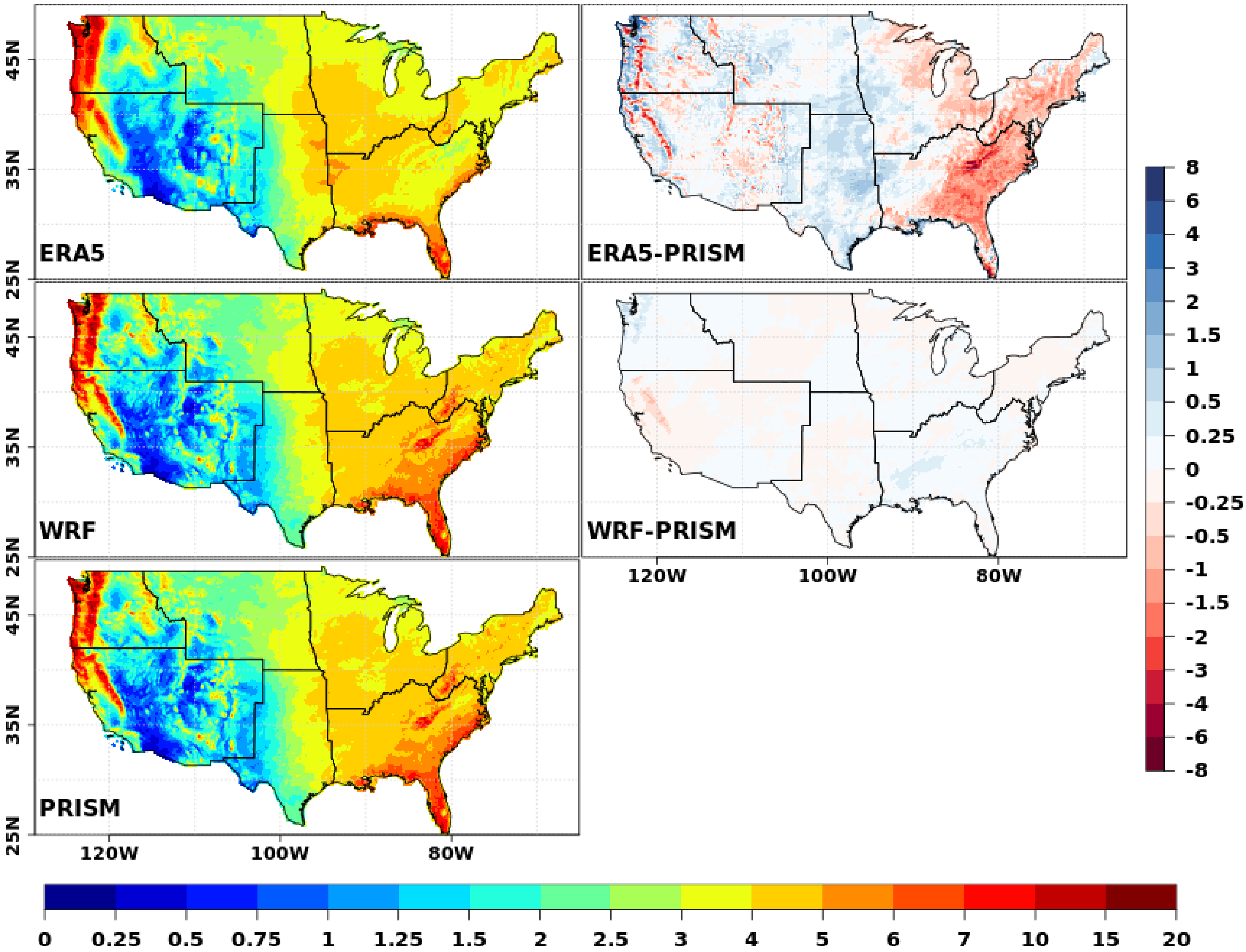

Figure 5. Magnitude of the monthly average precipitation peak estimated over 2001-2020. The left column shows the magnitude of the peak in each dataset and uses the color scale along the bottom edge of the figure. The right column shows biases in the magnitude and uses the color scale along the right edge of the figure. Units: mm/day.

https://doi.org/10.5194/egusphere-2022-1382
Preprint. Discussion started: 26 January 2023

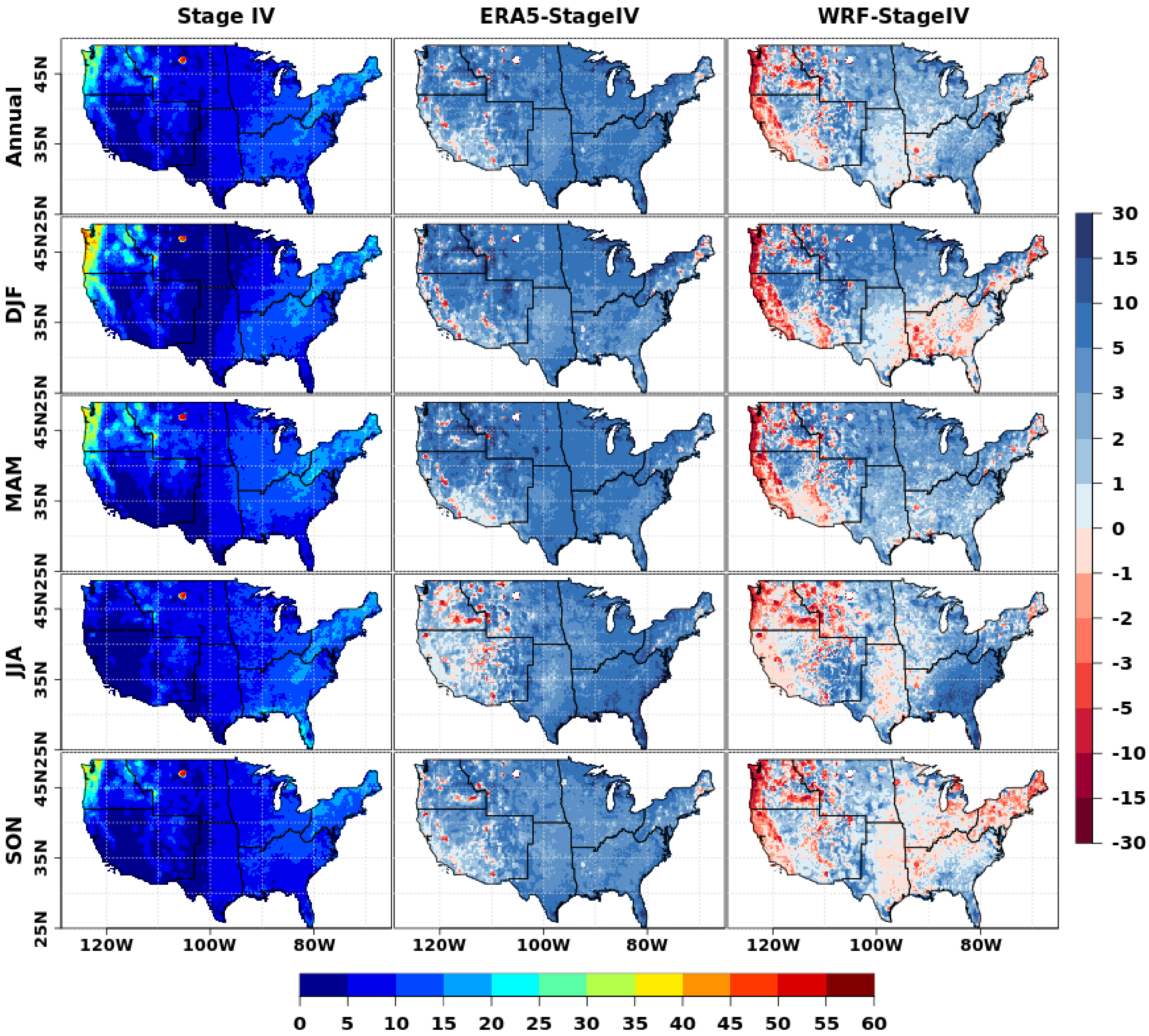

Figure 6. 3-hr precipitation frequency estimated over the 2003-2019. The left column shows the frequency in Stage IV data and uses the color scale along the bottom of the figure. The right two columns show differences in the precipitation frequency and use the color scale along the right edge of the figure. Units: %.

https://doi.org/10.5194/egusphere-2022-1382
Preprint. Discussion started: 26 January 2023

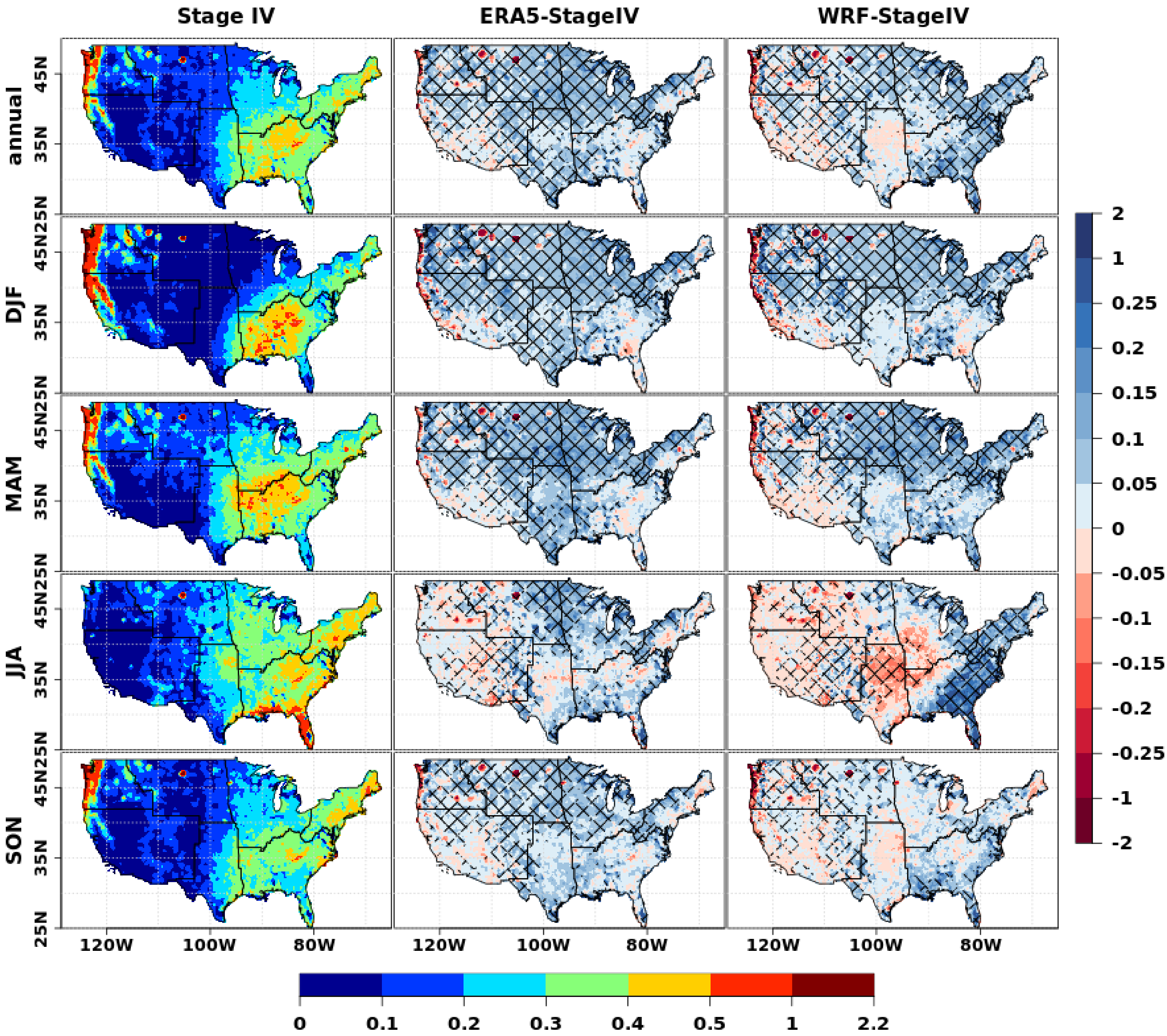

Figure 7. 3-hr precipitation mean estimated over the 2003-2019. The left column shows the mean in Stage IV data and uses the color scale along the bottom of the figure. The right two columns show differences in the mean and use the color scale along the right edge of the figure. Hatching denotes grid points where the differences are found to be significant at the 5% significance level based upon t-test. Units: mm/3hr.

https://doi.org/10.5194/egusphere-2022-1382
Preprint. Discussion started: 26 January 2023

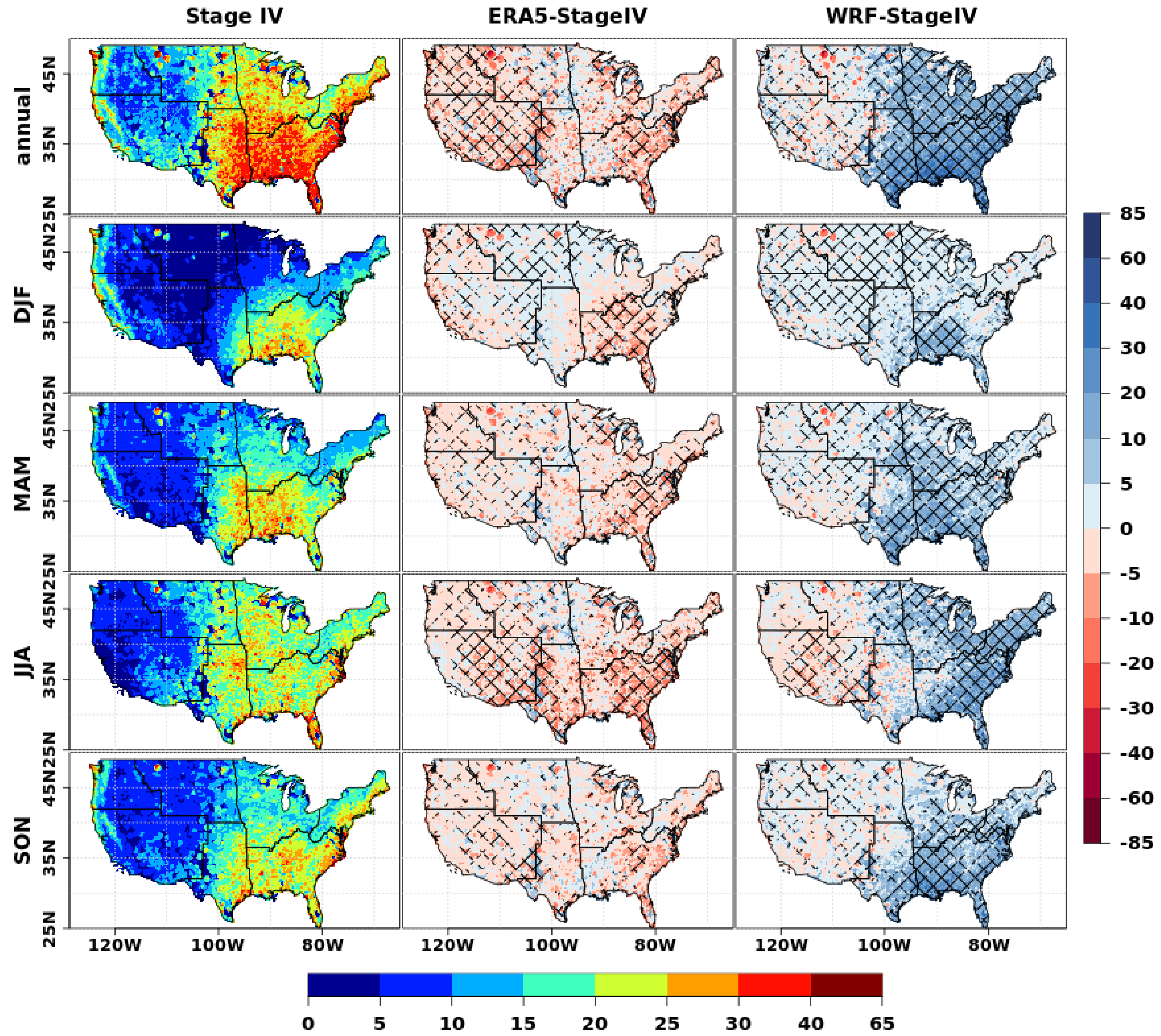

Figure 8. 3-hr precipitation maximum estimated over 2003-2019. The left column shows the mean in Stage IV data and uses the color scale along the bottom of the figure. The right two columns show differences in the mean and use the color scale along the right edge of the figure. Hatching denotes grid points where the differences are found to be significant at the 5% significance level based upon t-test. Units: mm/3hr.

https://doi.org/10.5194/egusphere-2022-1382
Preprint. Discussion started: 26 January 2023

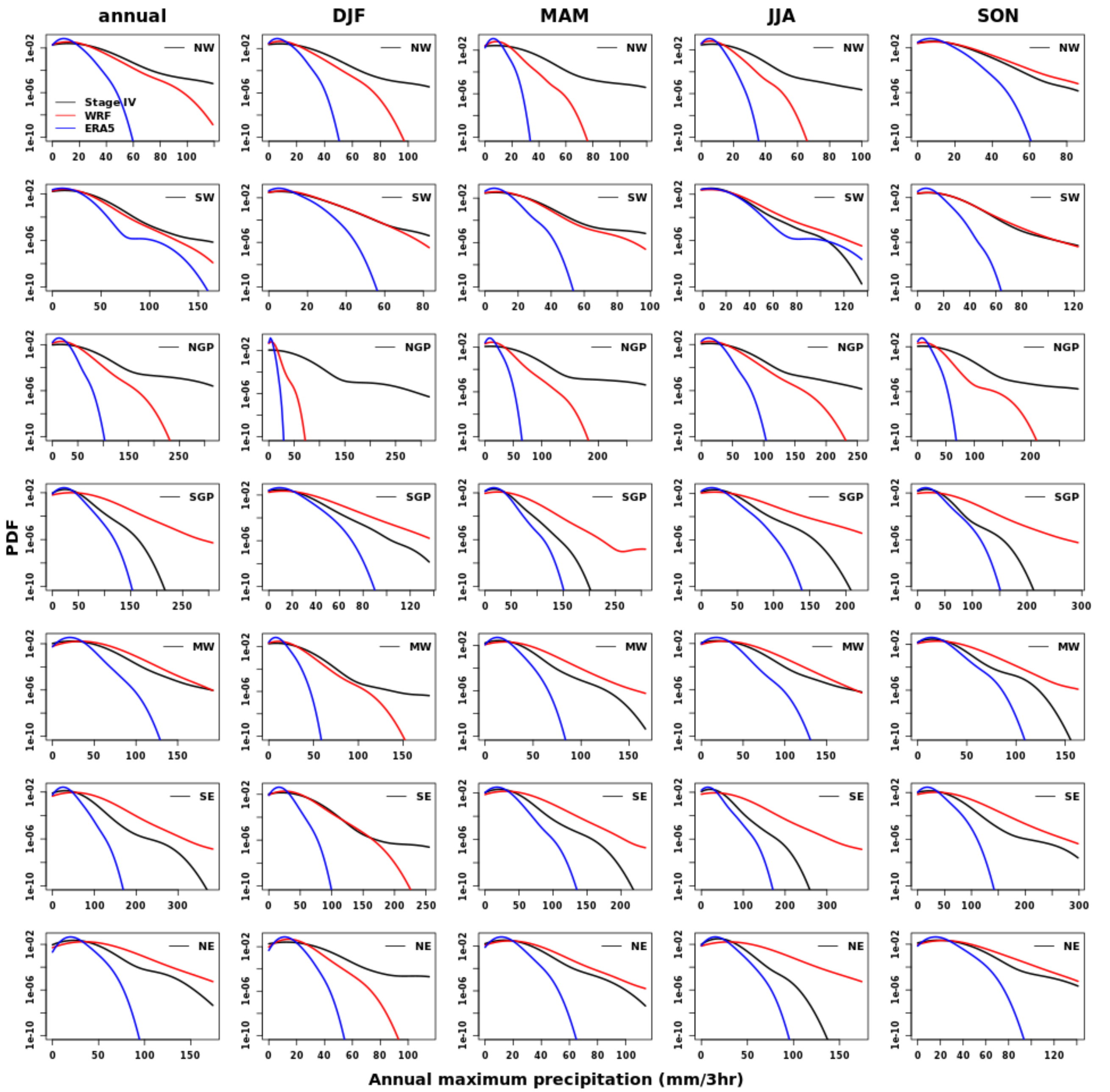

Figure 9. Probability density function (PDF) of 3-hr precipitation annual maximum estimated over 2003-2019. The Y-axis is plotted on log-scale.

https://doi.org/10.5194/egusphere-2022-1382
Preprint. Discussion started: 26 January 2023

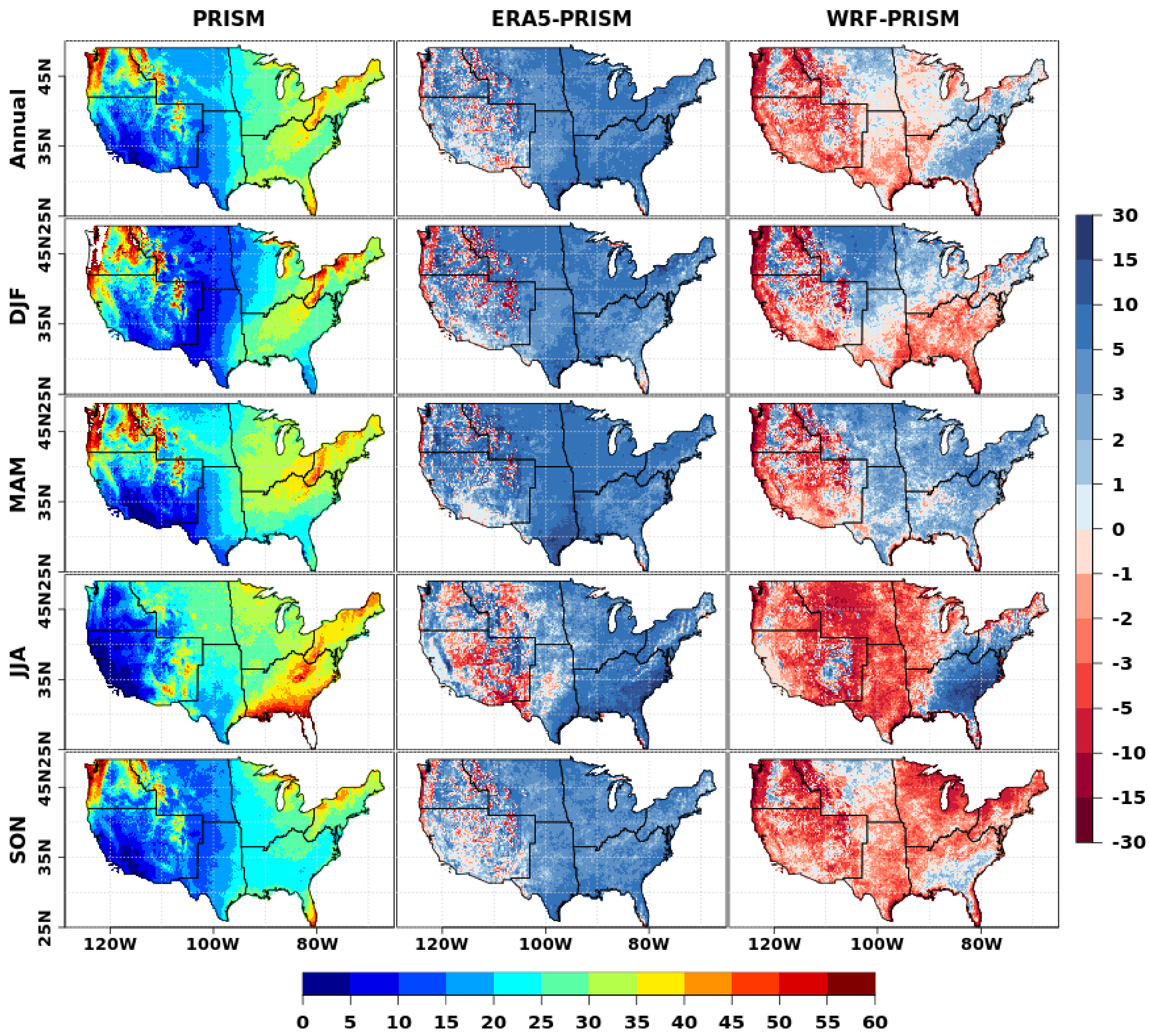

Figure 10. As Fig. 6 but for 24-hr precipitation frequency estimated over 2001-2020. Units: %

https://doi.org/10.5194/egusphere-2022-1382
Preprint. Discussion started: 26 January 2023

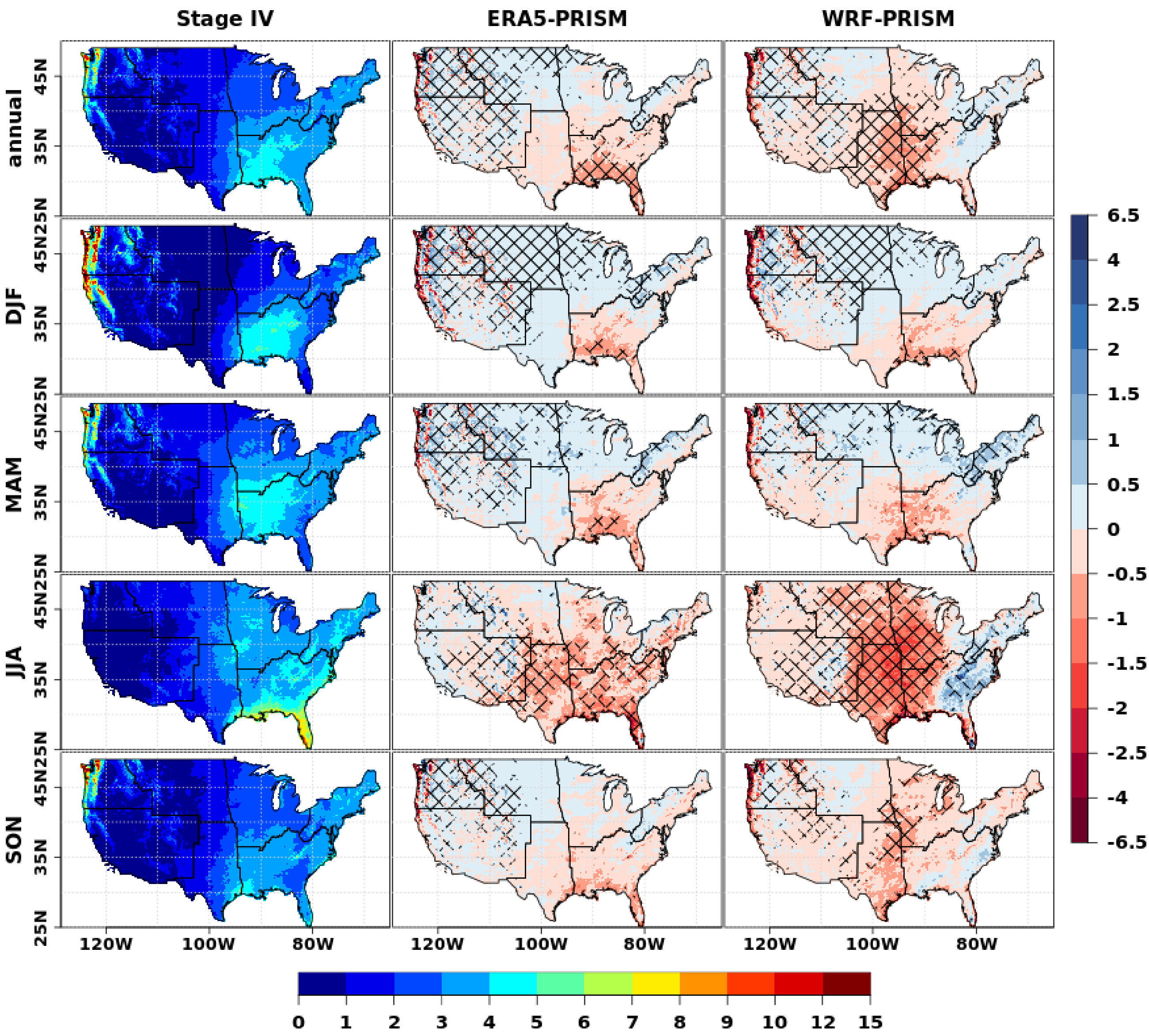

Figure 11. As Fig. 7 but for 24-hr precipitation mean estimated over 2001-2020. Units: mm/day.

https://doi.org/10.5194/egusphere-2022-1382
Preprint. Discussion started: 26 January 2023

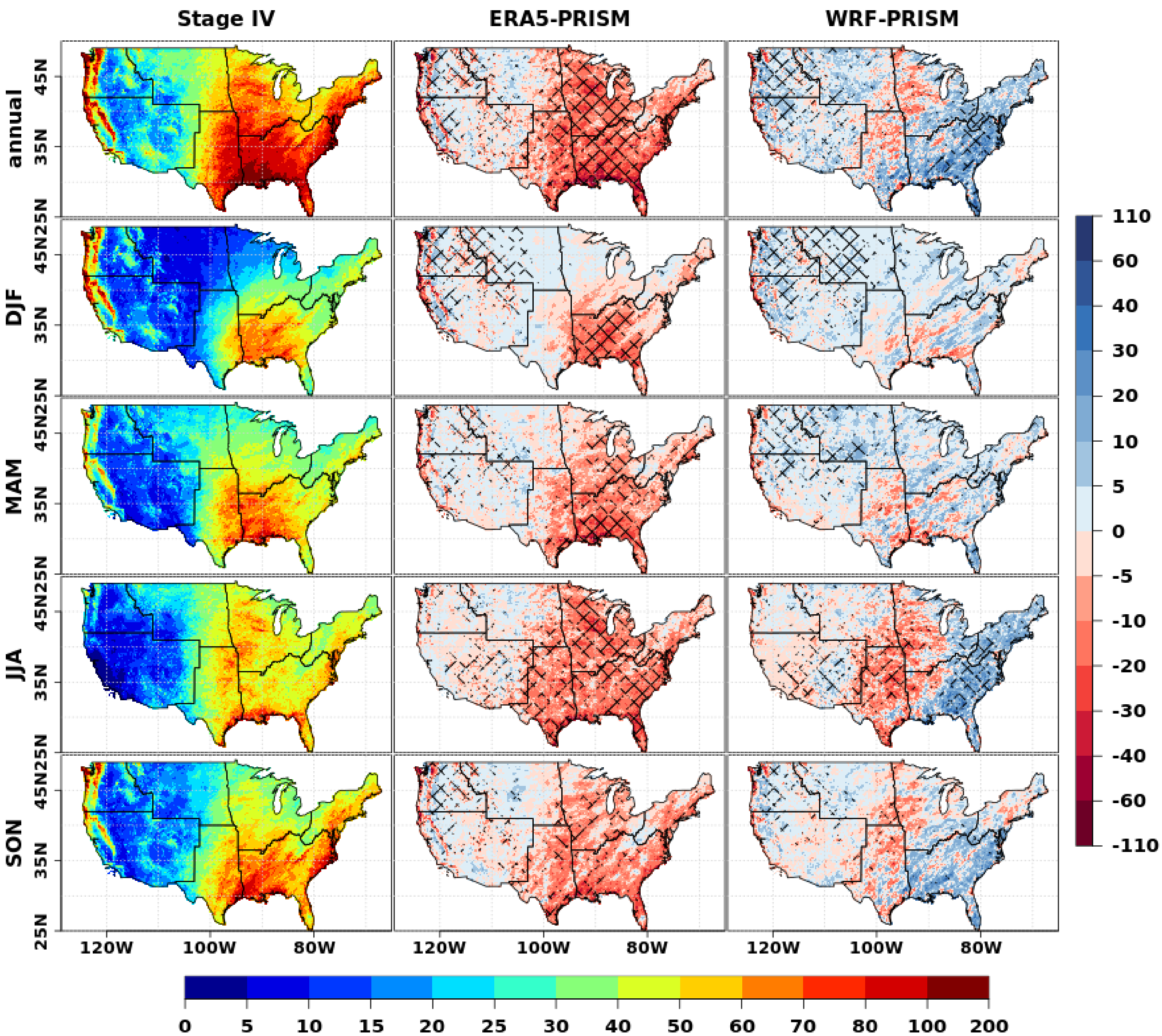

Figure 12. As Fig. 8 but for 24-hr precipitation maximum estimated over the 2001-2020. Units: mm/day.

https://doi.org/10.5194/egusphere-2022-1382
Preprint. Discussion started: 26 January 2023

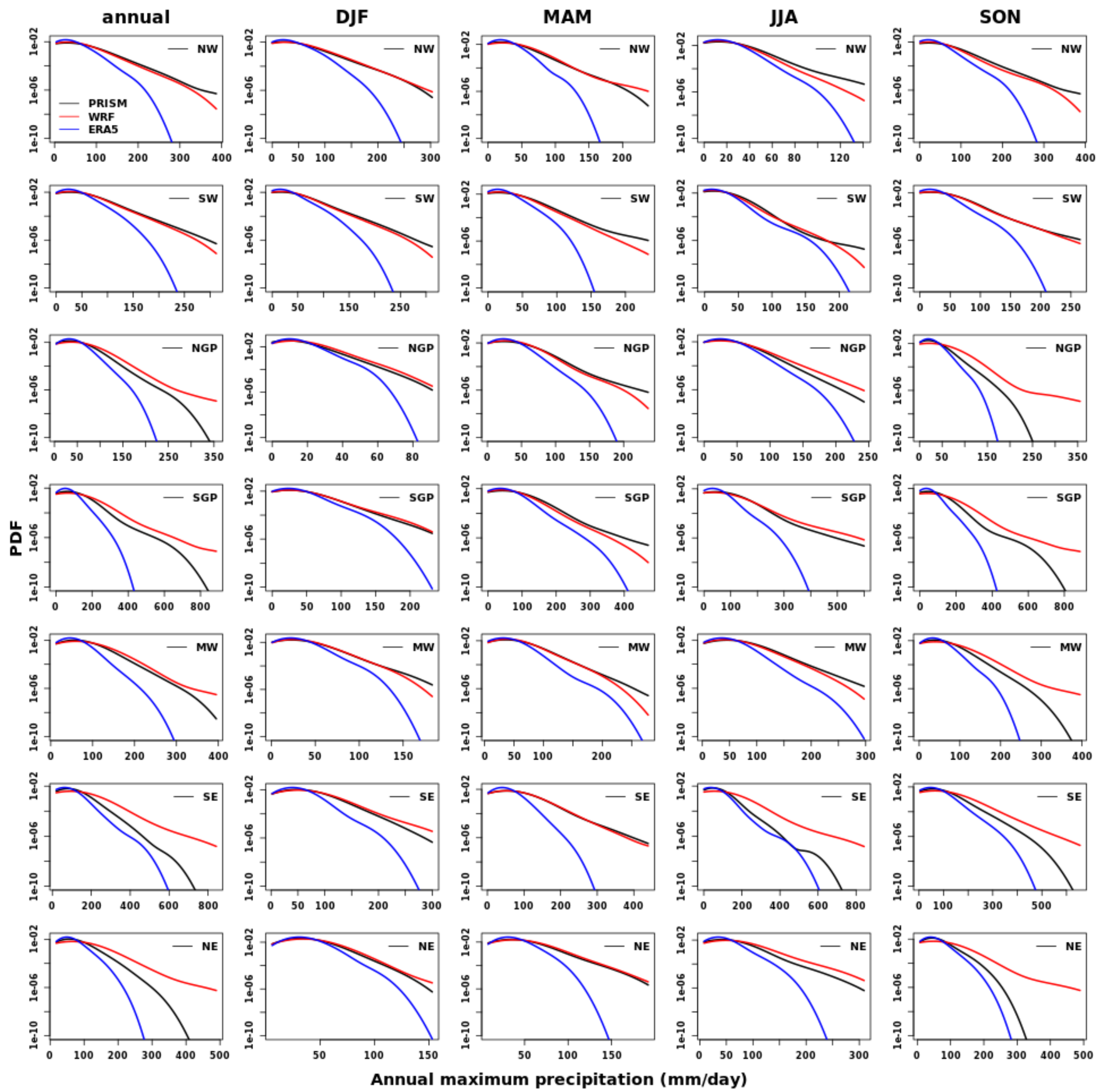

Figure 13. As Fig. 9 but for the PDF of 24-hr precipitation maximum estimated over 2001-2020.

https://doi.org/10.5194/egusphere-2022-1382
Preprint. Discussion started: 26 January 2023

Table 1. Regions where ERA5 or WRF precipitation (P) fidelity is subjectively better.

Precipitation parameter (observation-based dataset) <relevant Figure>	ERA5	WRF	Comments
Diurnal timing of peak P (Stage IV) < Fig. 2 >	The peak occurs earlier over much of the CONUS, especially along the northern boundaries of the Northern Great Plains (NGP) and west of the Great Lakes in the Midwest (MW).	Earlier peak over much of CONUS, better in NE. OEPC (overnight eastward progression of convection) too early in northern NGP, too late in SGP.	Generally larger biases are with OEPC in NGP & parts of: SGP and MW. Both datasets are too late for northern OEPC and too early for southern OEPC. (Note: 12 hrs late = 12 hrs early). Both are too early along NW coast.
Magnitude of JJA peak diurnal P (Stage IV) <Fig. 3>	Better over SE & SGP. Too wet over south FL & Rockies.	Too large over most of SE & less so over NE & eastern MW. Too dry over northern SGP. Better over Rockies.	ERA5 & WRF fine over NW & SW though the magnitude is smaller than elsewhere.
Timing of monthly average precipitation peak (PRISM) <Fig. 4>	Simulates the spatial pattern except over NE & Gulf regions.	Slightly better over SGP, NE, northern SE, & Great Basin.	NW, SW, NGP, MW, & southeastern SE good in both datasets.
Magnitude of the monthly average precipitation peak (PRISM) <Fig. 5>	Too dry over most of SE & NE, & eastern NW. Too wet over SGP, much of NGP, & coastal NW.	Generally better over whole CONUS	Both the magnitude and timing of the annual cycle are improved in WRF.
Annual 3-hr P frequency (Stage IV) <Fig. 6>	Generally too frequent (>5%) everywhere, less error over southern SW.	Better over NGP, MW, SGP, western SE. SW & NW generally better except not frequent enough along coastal & west-slopes of: NW & SW.	Both datasets too frequent (>5%) over most of: SE, MW, & NGP.
Seasonal 3-hr P frequency (Stage IV) <Fig. 6>	Seasons have similar excess as annual except JJA has reduced excess over most of SW & NW. Better at coast & western slopes in DJF, MAM, & SON.	Patterns differ from annual: western SW better during JJA. SGP worse during MAM. SE better in MAM & SON, too frequent during JJA.	ERA5 has frequent P throughout the year, WRF displays seasonal variation.
Annual 3-hr average P (Stage IV) <Fig. 7>	Generally too wet, except good in SE & southwestern SW.	Best over SGP. Worse over most of SE & NE. Too dry at NW coast. Generally, slightly smaller bias elsewhere.	seasonal biases in WRF over SGP are better except in JJA.

https://doi.org/10.5194/egusphere-2022-1382
Preprint. Discussion started: 26 January 2023

Table 1 (Contd . . .).

Precipitation parameter (observation-based dataset) <relevant Figure>	ERA5	WRF	Comments
Seasonal 3-hr average P (Stage IV) <Fig. 7>	MAM: slightly better in NE, SE, SW, & NW coast. JJA: better over SE, SGP, & NE. SON: better in SE, and better along NW coast.	MAM: SGP better. During JJA: SGP & western SE too dry, while eastern SE & all of NE are too wet. SON: better over NGP, MW, and interior SW	DJF similar in both, except NW coast better in ERA5. MAM similar over NGP & MW for both. Though opposite: SON good in both over SGP.
Annual 3-hr max P (Stage IV) <Fig. 8>	Generally too small over whole CONUS, especially eastern SE.	Better over most of NW, NGP, & SW. Much too wet over SGP, MW, SE, & NE.	Most larger values cover SE and eastern SGP.
Seasonal 3-hr max P (Stage IV) <Fig. 8>	Generally too small over CONUS though bias least during SON. Only notable area too wet is NGP during DJF. Worst bias during JJA over most of SE & border between SGP & SW.	Generally too wet over MW, NE, & SE though bias least during DJF. Worst biases during JJA too wet over most of MW, NE, & SE while too dry over interior SW. MAM and SON too wet over SE & southern SGP.	WRF shows wet bias in the eastern CONUS, ERA shows dry bias roughly everywhere.
Probability density function (PDF) of 3-hr max P (Stage IV) <Fig. 9>	3-hr max P values are severely underrepresented.	Much better representation. Large underestimation in NGP and overestimation in SGP	NGP and SGP are problematic regions for WRF
Annual 24-hr P frequency (PRISM) <Fig. 10>	Generally better over SW & coastal NW. Generally too frequent over NGP, SGP, MW, NE, & SE.	Generally better over NGP, MW, & NE. Too frequent over eastern SE. Much too infrequent over most of: NW, SW, SGP.	Highest observed over: NE, south FL, coast and mountains of NW & NGP.
Seasonal 24-hr P frequency (PRISM) <Fig. 10>	DJF better along coastal NW & most of SW. DJF, MAM, & SON: too frequent over NGP, MW, NE, SE, SGP, and most of: SW & NW.	DJF is better over most of MW, NE, & SGP. Coastal & mountainous: NW & SW are generally too infrequent during DJF, MAM, & SON. SE too infrequent during DJF but other seasons too frequent. JJA: much too infrequent over all but opposite bias over parts of SE & NE. SON: too infrequent over most of CONUS	Both datasets too infrequent along NW coast during DJF & SON, though ERA5 better there. Both too infrequent during JJA over most of SW.

https://doi.org/10.5194/egusphere-2022-1382
Preprint. Discussion started: 26 January 2023

Table 1 (Contd . . .).

Precipitation parameter (observation-based dataset) <relevant Figure>	ERA5	WRF	Comments
Annual 24-hr average P (PRISM) <Fig. 11>	Worse biases (dry) over southern SE.	Worse biases (dry) over western SE and most of SGP.	observed peak values over western SE and coastal NW. Datasets generally similar except SE, SGP, & coastal NW where WRF has greater dry bias.
Seasonal 24-hr average P (PRISM) <Fig. 11>	MAM & SON biases generally similar to DJF. JJA has largest biases (dry) covering all of: SGP & SE & much of: MW & NE. JJA & SON better over NGP, MW, SGP, & western SE.	MAM bias similar to DJF. Largest bias (dry) is during JJA and covers SGP, most of: MW & NGP, and western SE. SON: coastal SE is better.	DJF: similar in both datasets with greater bias along coast of NW, & Gulf of Mexico coast of SE. Largest seasonal values are at coastal NW during DJF; ERA5 captures this better. Secondary maximum during JJA covers FL and SE Gulf of Mexico coast; both datasets underestimate these larger values.
Annual 24-hr max P (PRISM) <Fig. 12>	General dry bias over SGP, MW, SE, & NE. Slightly better over NW & SW.	Wet bias over most of SE, NE, eastern MW, & parts of: SW, NGP, & NW.	Datasets do well over NW, NGP, & SW. They have opposite biases over most of SE, NE, MW, & southern SGP.
Seasonal 24-hr max P (PRISM) <Fig. 12>	DJF: dry bias mainly in SE. MAM, JJA, & SON: dry bias across SGP, SE, MW, & NE.	DJF: better over SE. MAM & SON: better over most of: SGP, SE, MW, NE. JJA: wet bias over: NE & eastern and southern SE.	Performance similar over SW, NW, & NGP. Both have large dry bias over SGP during JJA. Bias generally smaller over SW, NW, and NGP, but so are the observed means.
Probability density function (PDF) of 24-hr max P (Stage IV) <Fig. 13>	24-hr max P values are severely underrepresented.	Much better representation.	24-hr PDF representation is better than the 3-hr PDF in WRF.